insurance program in Japan. They have been shown to be effective in decreasing serum HBV DNA and alanine aminotransferase (ALT) levels, improving hepatic reservation and liver histology.[5–11] It has also been reported that LVD decreases the risk of developing liver failure and hepatocarcinogenesis.[12,13]

A high serum HBV DNA load has been shown to be the most critical risk factor for HCC in HBV carriers.[14] Therefore, current treatment guidelines for patients with CHB or cirrhosis stress the importance of suppression of the serum HBV DNA load by antiviral treatment including NA administration in order to minimize the risk of liver disease progression and hepatocarcinogenesis.[15–18] However, the long-term effect of NA treatment on prognosis, especially on development of HCC in patients with CHB or cirrhosis, has not been fully elucidated.

Therefore, we designed this prospective cohort study to elucidate the virological and biochemical treatment effects and the long-term prognosis – particularly with respect to development of HCC – of patients with CHB or cirrhosis, who were started on LVD treatment, with or without co-administration with ADV, and ETV treatment.

METHODS

Study design

THIS STUDY WAS a prospective, non-randomized open-label cohort study on NA treatment for patients with CHB or cirrhosis without complications or past history of HCC. It was started as a study on LVD treatment for CHB or cirrhosis in November 2000, and then later modified to include ETV treatment when ETV was approved for coverage by the health insurance program and became commercially available in Japan in September 2006. This study was designed and performed in accordance with the provisions of the Declaration of Helsinki and Good Clinical Practice guidelines. The study was approved by the Institutional Committee for Human Rights. This study was also registered for the University Hospital Medical Information Network CTR system (ID: UMIN 000000594).

Subject population

The eligible patients were men and women aged 20 years or older, diagnosed with CHB or cirrhosis, without previous NA administration, and without complications or past history of HCC. The diagnosis of CHB and cirrhosis was made by positive hepatitis Bs antigen and positive serum HBV DNA with elevated serum ALT. The indication criteria for NA included serum HBV DNA greater than 5 log copies/mL with an elevated ALT level over twice the upper normal limit (ULN) or with complications of hepatic insufficiency, such as jaundice, ascites or encephalopathy.

The diagnosis of cirrhosis was confirmed by liver histology, clinical signs (encephalopathy or ascites), evidence of esophagogastric varices by endoscopy, or imaging modalities such as ultrasonography (US), computed tomography (CT) or magnetic resonance imaging (MRI).

All patients were deemed to be without complications of HCC by US, CT or MRI performed within 3 months before enrollment. Patients with acute hepatitis, fulminant hepatitis, alcoholic liver injury, co-infection with hepatitis C virus, autoimmune hepatitis, primary biliary cirrhosis, non-alcoholic steatohepatitis or hereditary liver diseases were excluded. All patients were informed of the aim and methodology of the study, received a written synopsis and gave their written consent to participate. The patients were started on LVD 100 mg/day or ETV 0.5 mg/day p.o. Some patients who had been started on ETV as participants of ETV phase II clinical study in Japan were also enrolled in this study.[9] In this paper, the study population consisted of the subjects enrolled between November 2000 and December 2009, and the patients' data between enrollment and November 2010 were used.

Patient follow up

The patients were followed up every month with a medical consultation and the following blood examinations: serum albumin, total bilirubin, aspartate AST, ALT, prothrombin time (PT%), platelet count (Plt), hepatitis B e-antigen (HBeAg), anti-HBe antibody by chemiluminescence immunoassay (Chemi-luminescent Immunoassay; Abbott Japan, Tokyo), and serum HBV DNA by polymerase chain reaction (PCR) assay (Roche Amplicor PCR assay; Roche Diagnostics, Tokyo, Japan), real-time PCR assay (Cobas TaqMan HBV Auto; Roche Diagnostics), or transcription-mediated amplification (TMA) assay (Chugai Diagnostics, Tokyo, USA). The detection ranges for the HBV DNA assay of PCR, real-time PCR and TMA were from 2.6–7.6 log copies/mL, from 1.8–8.8 log copies/mL and from 3.7–8.7 log genome equivalent/mL, respectively, permitting close determination with nearly equal quantitative accuracies. Levels of HBV DNA under the lower limit of normal (LLN) or over the ULN were assigned the value of the LLN or the ULN, respectively, in statistical analysis.

Drug resistance was confirmed by virological breakthrough and defined as an increase in serum HBV DNA by more than 1 log copy/mL greater than nadir. If virological breakthrough developed in patients receiving LVD, co-administration of ADV 10 mg/day or change to ETV 1.0 mg/day was selected. If virological breakthrough developed in patients receiving ETV, ETV was stopped and changed to co-administration of LVD 100 mg/day and ADV 10 mg/day.

Surveillance and diagnosis of HCC

As surveillance for HCC, α-fetoprotein (AFP) by electrochemiluminescent immunoassay (Roche Diagnostics) and des-g-carboxy prothrombin (DCP) by electrochemiluminescent immunoassay (Sanko, Tokyo, Japan) were measured alternately every month. Image diagnosis by US, dynamic enhanced CT or dynamic enhanced MRI was performed every 6 months in CH patients and every 3 months in cirrhosis patients. If elevation of AFP or DCP was observed, imaging diagnosis was performed within a month. Diagnosis of HCC was confirmed by the finding of enhanced arterial contrast uptake followed by washout in the portal venous phase and equivalent phase by dynamic enhanced CT or dynamic enhanced MRI, or histologically by fine-needle tumor biopsy. The methods used for the confirmation of diagnosis and staging of HCC conformed to the standards by Liver Cancer Study Group of Japan.[19]

End-points

The primary end-point was the development of HCC. Secondary end-points included changes in serum HBV DNA, HBeAg, AST, ALT, serum albumin, PT%, AFP, DCP, Plt and Child–Turcotte–Pugh class between baseline and the latest visit. Seroconversion was defined as loss of HBeAg and development of anti-HBe. In the case of patients who developed HCC during the study period, the last data gathered before the first detection of HCC by imaging were adopted as the latest data. In the patients who developed HCC, the size, number and stage of tumors were also estimated. The sensitivity and specificity of AFP and DCP were estimated using the values at diagnosis of HCC for the patients who developed HCC, and those at the latest visit for patients without HCC. Only the specificity of AFP and DCP, without sensitivity, was estimated at baseline using the values of AFP and DCP at baseline, when no patients had yet developed HCC.

Statistical analysis

Parameters represented by continuous variables were expressed as the median and range (minimum and maximum). Parameters at baseline were compared between ETV patients and LVD patients by Mann–Whitney *U*-test for continuous variables and by χ^2-test for categorical data. Each parameter at the latest visit was compared with the corresponding one at baseline by Mann–Whitney *U*-test for continuous variables and by χ^2-test for categorical data. The incidence of HCC development was estimated by Kaplan–Meier analysis, and compared between the patients with CH and cirrhosis, and between the patients started on ETV and those administrated LVD, using a log–rank test. Receiver–operator curves (ROC) for serum AFP and DCP were estimated to search for the optimal cut-off value to distinguish between the patients with and without HCC. A *P*-value of less than 0.05 was considered statistically significant. Statistical analysis was performed with JMP software ver. 5.01J.

RESULTS

Study populations and baseline characteristics (Table 1)

A TOTAL OF 256 patients were enrolled in this study. ETV and LVD were administrated to 129 and 127 patients, respectively, as the first-line NA. The baseline characteristics and demographics of all patients, the ETV group and the LVD group, are shown in Table 1. All patients were Japanese, and consisted of 179 men and 77 women, with a median age of 50 years. The median follow-up period was 4.25 years in all patients, 2.96 years in ETV patients and 5.97 years in LVD patients.

As for viral markers, the median serum HBV DNA level was 7.0 log copies/mL and HBeAg was positive in 132 patients of the total patient group, with no significant difference between the ETV and LVD groups.

The clinical diagnosis in all patients was CH in 194 and cirrhosis in 62 patients and there was no significant difference in distribution between the ETV and LVD groups. In the 62 patients with cirrhosis, the Child–Turcotte–Pugh class was A, B and C in 43, 16 and three patients, respectively. The serum albumin concentration, PT% and Plt were significantly lower in the LVD group than the ETV group, indicating that hepatic reservation was somewhat lower in the LVD group.

Liver biopsy was performed and assessed using the New Inuyama Classification system in 166 patients in

Table 1 Baseline characteristics of the subjects

	All ($n = 256$)	ETV ($n = 129$)	LVD ($n = 127$)	*P*-value
Sex (male/female)†	179/77	86/43	93/34	0.2964
Age (years)‡	50 (22–88)	51 (26–88)	50 (22–81)	0.4369
Follow-up period (years)‡	4.25 (0.41–10.0)	2.86 (0.41–7.47)	5.97 (0.51–10.0)	<0.0001*
Fibrosis stage (1/2/3/4)†	42/57/50/17	23/31/21/6	19/26/29/11	0.2665
Activity grade (1/2/3)†	49/80/37	29/34/18	20/46/19	0.2276
Clinical diagnosis (CH/LC)†	194/62	101/28	93/34	0.2934
CTP class A/B/C (in LC patients)†	43/16/3	23/4/1	20/12/2	0.1253
HBV DNA (log copies/mL)‡	7.0 (2.6–8.8)	6.8 (2.6–8.8)	7.3 (3.0–8.7)	0.1763
HBeAg (positive/negative)†	132/124	67/62	65/62	0.952
Total bilirubin (mg/dL)‡	0.87 (0.2–22.67)	0.86 (0.2–5.19)	0.875 (0.38–22.67)	0.0617
Albumin (g/dL)‡	4.0 (2.07–5.0)	4.1 (2.3–5.0)	3.96 (2.0–5.0)	0.0090*
AST (IU/L)‡	66 (12–1216)	61 (12–811)	73 (19–1216)	0.0427*
ALT (IU/L)‡	87 (13–1660)	82 (13–1250)	96 (14–1660)	0.0569
Platelet count (×104/μL)‡	14.0 (3.9–47.2)	17.5 (3.5–32.8)	15.7 (3.6–52.2)	<0.001*
Prothrombin time (%)‡	88.0 (27.8–132.0)	93.0 (58.0–132.0)	83.0 (27.8–122.6)	<0.001*
AFP (ng/mL)‡	5.8 (1.4–1057.1)	5.7 (1.4–820.6)	5.8 (1.4–1057.1)	0.839
DCP (mAU/mL)‡	20.0 (6.0–145.0)	19.0 (6.0–145.0)	20.0 (10.0–89.0)	0.2282

*Different between ETV and LVD groups with statistical significance.
†Values are numerical and analyzed by χ^2-test.
‡Values are median (range) and analyzed by Mann–Whitney *U*-test.
AFP, α-fetoprotein; ALT, alanine aminotransferase; AST, aspartate aminotransferase; CH, chronic hepatitis; CTP, Child–Turcotte–Pugh; DCP, des-γ-carboxy prothrombin; ETV, entecavir; HBeAg, hepatitis B e-antigen; LC, liver cirrhosis; LVD, lamivudine.

total. Fibrosis stages of 1, 2, 3 and 4 were observed in 42, 57, 50 and 17 patients, and activity grades of 1, 2 and 3 were observed in 49, 80 and 37 patients in total, both with no significant difference between the ETV and LVD groups.

As for tumor markers, the median AFP was 5.8 ng/mL and the median DCP was 20.0 mAU/mL, and neither marker was significantly different between the ETV and LVD groups. The complication of HCC was neglected in all patients by the inclusion criteria.

Changes in virological and biochemical markers (Fig. 1)

Median serum HBV DNA dropped significantly from 7.0 log copies/mL at baseline to 2.1 log copies/mL at the latest visit ($P < 0.0001$) (Fig. 1a). Serum HBV DNA was under the LLN in 220 out of 256 cases at the latest visit. There was no difference in the latest serum HBV DNA or the rate of decline between the ETV and LVD groups. Among the 132 patients with positive HBeAg at baseline, HBeAg seroconversion was observed in 48 patients (36.4%) after a median period of 4.25 years.

Median serum albumin was significantly elevated from 4.0 g/dL at baseline to 4.4 g/dL at the latest visit ($P < 0.0001$) (Fig. 1b). The median AST dropped from 66 to 22 IU/L ($P < 0.0001$), and the median ALT dropped from 87 to 19 IU/L ($P < 0.0001$) (Fig. 1c,d). The median PT% was elevated from 88% to 100% ($P < 0.0001$), and the median Plt increased from 14.0 to $16.7 \times 10^4/\mu L$ ($P < 0.0001$) (Fig. 1e,f). By subgroup

Figure 1 Comparison of the measured parameters between baseline and the latest visit (a–f) by Mann–Whitney *U*-test for continuous valuables and (g) by χ^2-test for Child–Turcotte–Pugh class distribution. (a) Median serum hepatitis B virus (HBV) DNA dropped significantly from 7.0 log copies/mL at baseline to 2.1 log copies/mL at the latest visit ($P < 0.0001$). (b) Median serum albumin was significantly elevated from 4.0 g/dL at baseline to 4.4 g/dL at the latest visit ($P < 0.0001$). (c) Median aspartate aminotransferase (AST) dropped significantly from 66 IU/L at baseline to 22 IU/L at the latest visit ($P < 0.0001$). (d) Median alanine aminotransferase (ALT) dropped significantly from 87 IU/L at baseline to 19 IU/L at the latest visit ($P < 0.0001$). (e) Median prothrombin time (PT) was significantly elevated from 88% at baseline to 100% at the latest visit ($P < 0.0001$). (f) Median platelet count (PLT) increased significantly from 14.0 at baseline to $16.7 \times 10^4/\mu L$ at the latest visit ($P < 0.0001$). (g) In the 62 patients with cirrhosis, the distribution of Child–Turcotte–Pugh class A, B and C changed from 43, 16 and three at baseline to 56, six and zero at the latest visit, with significant difference by χ^2-test ($P = 0.0173$).

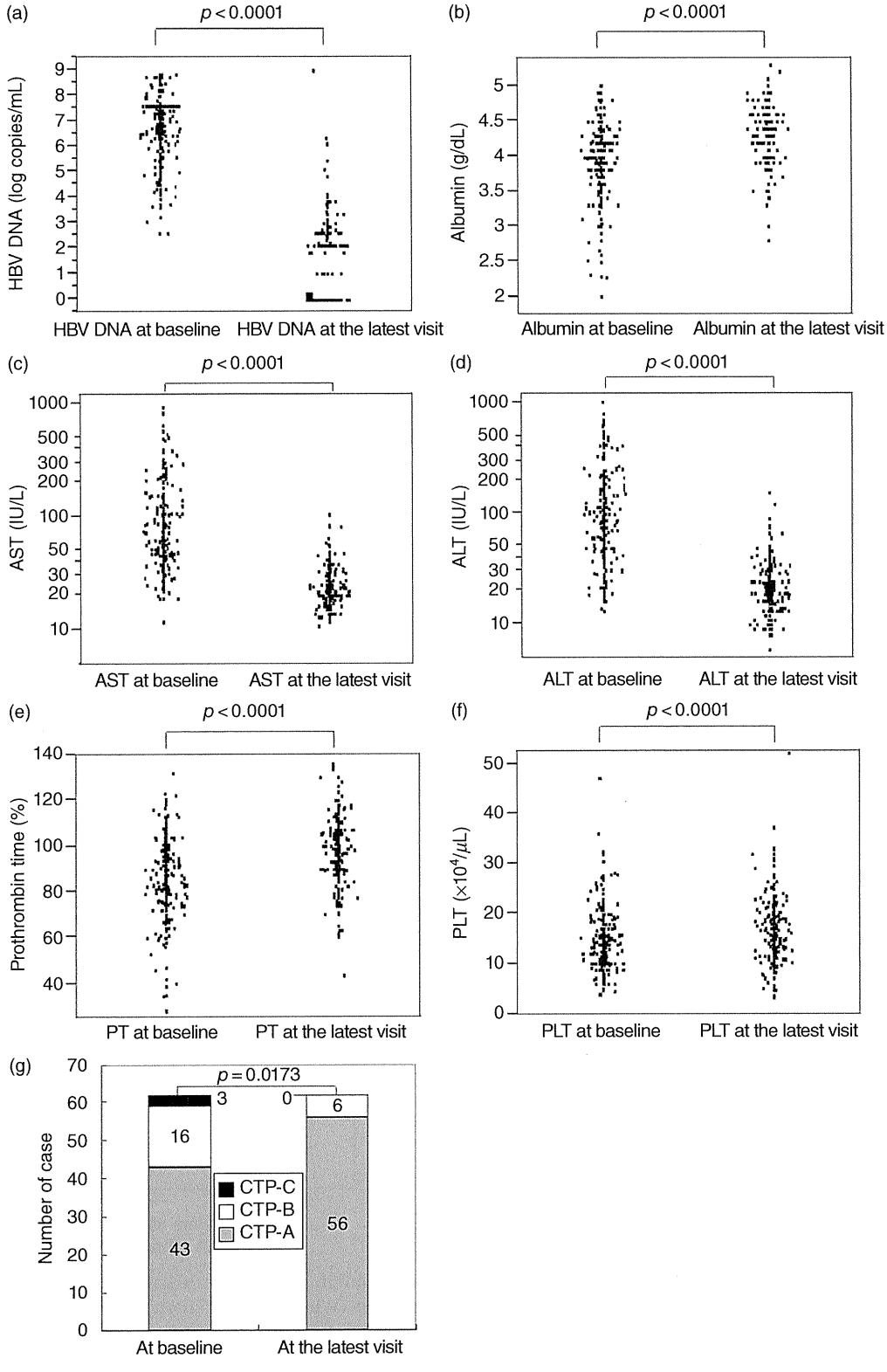

analysis, these parameters changed similarly and significantly in both the ETV and LVD groups. In the 62 patients with cirrhosis, the distribution of Child–Turcotte–Pugh class A, B and C changed from 43, 16 and three at baseline to 56, six and zero at the latest visit, and the change in each class was significantly different by χ^2-test ($P = 0.0173$) (Fig. 1g).

Drug resistance

Among the 127 patients of the LVD group, virological resistance cumulatively developed in 60 patients during the follow-up period; co-administration of ADV was selected in 53 of these patients, and change to ETV was selected in the other seven patients. In the 129 patients of the ETV group, resistance to ETV developed in one patient, and the protocol was changed to co-administration of LVD and ADV for this patient.

Tumor markers (Fig. 2)

Median AFP dropped significantly from 5.8 ng/mL at baseline to 2.9 ng/mL at the latest visit without or before development of HCC ($P < 0.0001$) in both the ETV and LVD groups (Fig. 2a). There was no significant difference in median DCP between baseline (20.0 mAU/mL) and the latest visit (19.0 mAU/mL) (Fig. 2b). Median serum AFP levels changed from 5.8 ng/mL at baseline to 5.1, 3.9, 3.1 and 2.8 ng/mL at months 2, 4, 6 and 8 after NA treatment (Fig. 2c). In patients who developed HCC in the follow-up period, median AFP levels were 4.9, 5.3 and 5.4 ng/mL at months 6, 4 and 2 before diagnosis of HCC, and 6.6 ng/mL at diagnosis of HCC (Fig. 2d).

Development and characteristics of HCC (Table 2, Fig. 3)

During the follow-up period, HCC developed in 35 out of the total 256 patients, or 11 patients from the ETV

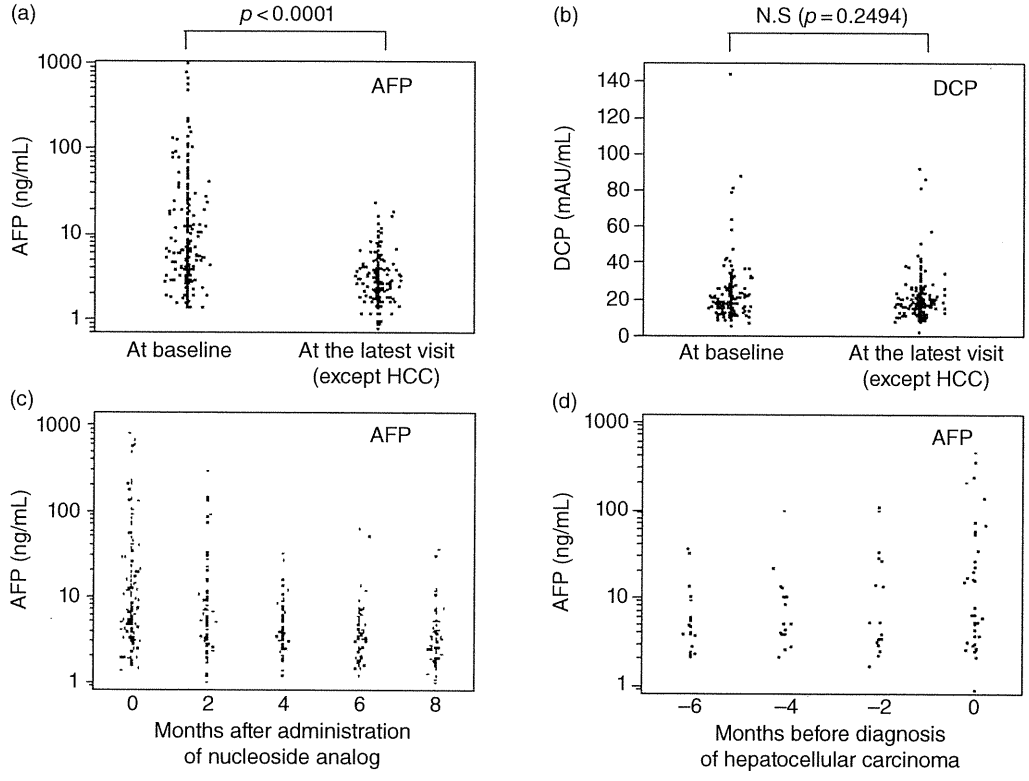

Figure 2 Changes in serum α-fetoprotein (AFP) and des-γ-carboxy prothrombin (DCP). (a) Median AFP dropped significantly from 5.8 ng/mL at baseline to 2.9 ng/mL at the latest visit ($P < 0.0001$ by Mann–Whitney *U*-test). (b) Median DCP at the latest visit, 19.0 mAU/mL, was not changed significantly from that at baseline, 20.0 mAU/mL ($P = 0.2494$ by Mann–Whitney *U*-test). (c) Median AFP levels changed from 5.8 ng/mL at baseline, to 5.1, 3.9, 3.1 and 2.8 ng/mL at months 2, 4, 6 and 8 after NA treatment. (d) In the patients who developed hepatocellular carcinoma (HCC), median AFP levels were 4.9, 5.3 and 5.4 ng/mL at months 6, 4 and 2 before diagnosis of HCC, and 6.6 ng/mL at diagnosis of HCC.

Table 2 Data at development of hepatocellular carcinoma

	$n = 35$
Background (CH/LC)†	14/21
NA (ETV/LVD)†	11/24
Duration of NA administration (years)‡	4.25 (0.4–10.0)
Size (cm)‡	1.9 (0.9–3.2)
Number (1/2/3)†	21/10/4
Stage 1/2/3/4A†	15/14/5/1
Treatment (Hr/RFA/TACE/PMCT)†	18/14/2/1
AFP (ng/mL)‡	6.6 (0.9–459)
DCP (mAU/mL)‡	27.0 (10–456)

†Values are numerical.
‡Values are median (range).
AFP, α-fetoprotein; CH, chronic hepatitis; DCP, des-γ-carboxy prothrombin; ETV, entecavir; Hr, hepatic resection; LC, liver cirrhosis; LVD, lamivudine; NA, nucleoside analog; PMCT, percutaneous microwave coagulation therapy; RFA, radiofrequency ablation; TACE, transcatheter arterial chemoembolization.

group and 24 patients from the LVD group. The background liver disease in these 35 patients at baseline was CH in 14 patients and cirrhosis in 21 patients. The mean duration from start of NA administration to HCC development was 4.25 years in total (Table 2). The cumulative incidence of HCC development at years 1, 3, 5, 7 and 10 in the all patients estimated by Kaplan–Meier analysis was 3.2%, 6.9%, 12.4%, 16.8% and 34.0%, respectively (Fig. 3a). It was 1.6%, 3.5%, 3.5%, 7.1% and 29.6% in CH, and 8.1%, 17.5%, 43.2%, 46.7% and 53.4% in cirrhosis patients, respectively, and the incidence in patients with cirrhosis was significantly higher than that in the patients with CH ($P < 0.0001$) (Fig. 3b). There was no difference in HCC development between the ETV group and LVD group ($P = 0.680$) (Fig. 3c). The cumulative incidence of HCC development was significantly ($P = 0.0352$) higher in patients who developed LVD resistance in the follow-up period, as compared with patients without LVD resistance (Fig. 3d).

The characteristics of HCC at diagnosis were as follows: the median diameter was 1.9 cm (ranging 0.9–3.2 cm), the number of tumors was 1, 2 and 3 in 21, 10 and four cases, and the tumor stage was 1, 2, 3 and 4A in 15, 14, five and one case, respectively. Treatment of HCC consisted of hepatic resection in 18 patients, radiofrequency ablation (RFA) in 14 patients, transcatheter arterial chemoembolization in two patients and percutaneous microwave coagulation therapy in one patient. The median AFP value at diagnosis of HCC was 6.6 ng/mL (as described previously), ranging from 0.9–459. The median DCP value at diagnosis of HCC was 27.0 mAU/mL, ranging from 10–456 (Table 2). There was no significant difference in these characteristics between the ETV and LVD groups.

Sensitivity and specificity of AFP and DCP (Table 3, Fig. 4)

Receiver–operator curve analysis indicated that the area under the curve of AFP was 0.797 and that of DCP was 0.736 (Fig. 4). ROC analysis suggested that an AFP value of approximately 10 ng/mL and DCP value of approximately 40 mAU/mL provided an optimal balance between sensitivity and specificity. The sensitivity and specificity of AFP by the cut-off value of 10 ng/mL was 45.7% and 97.3%, respectively, at diagnosis of HCC or at the latest visit. At baseline, the specificity of AFP by the cut-off value of 10 ng/mL was 64.4%. The sensitivity and specificity of DCP by the cut-off value of 40 mAU/mL was 33.3% and 96.2%, respectively, at diagnosis of HCC or at the latest visit. At baseline, the specificity of DCP was 95.1% by the cut-off value of 40 mAU/mL. (The sensitivity of AFP and DCP could not be estimated at baseline when all patients were without complication and/or past history of HCC.)

Using the combination of AFP and DCP, the sensitivity (AFP >10 ng/mL and/or DCP >40 mAU/mL) was 64.7%, and the specificity (AFP ≤10 ng/mL and DCP ≤40 mAU/mL) was 93.4%. At baseline, the specificity was 74.5%.

DISCUSSION

ALTHOUGH ANTI-HBV NA have a potent antiviral activity,[5–11] they cannot delete the HBV cccDNA template. Therefore, the aim of NA treatment is to realize a long-term improvement in the outcome of patients by sustained suppression of HBV proliferation and disease progression. The present study showed that NA treatment continuously exerted long-lasting effects on viral suppression, control of disease activity and improvement of hepatic reservation. Namely, median serum HBV DNA dropped to 2.1 log copies/mL, and HBV DNA was under the LLN in 220 out of 256 cases at the latest visit. The activity of liver disease was also suppressed, as shown by the reduction and normalization of AST and ALT. Hepatic reservation was significantly improved, as shown by the elevation in serum albumin concentration and PT%, and the Child–Turcotte–Pugh class was improved in the majority of patients with cirrhosis. It therefore seems reasonable to

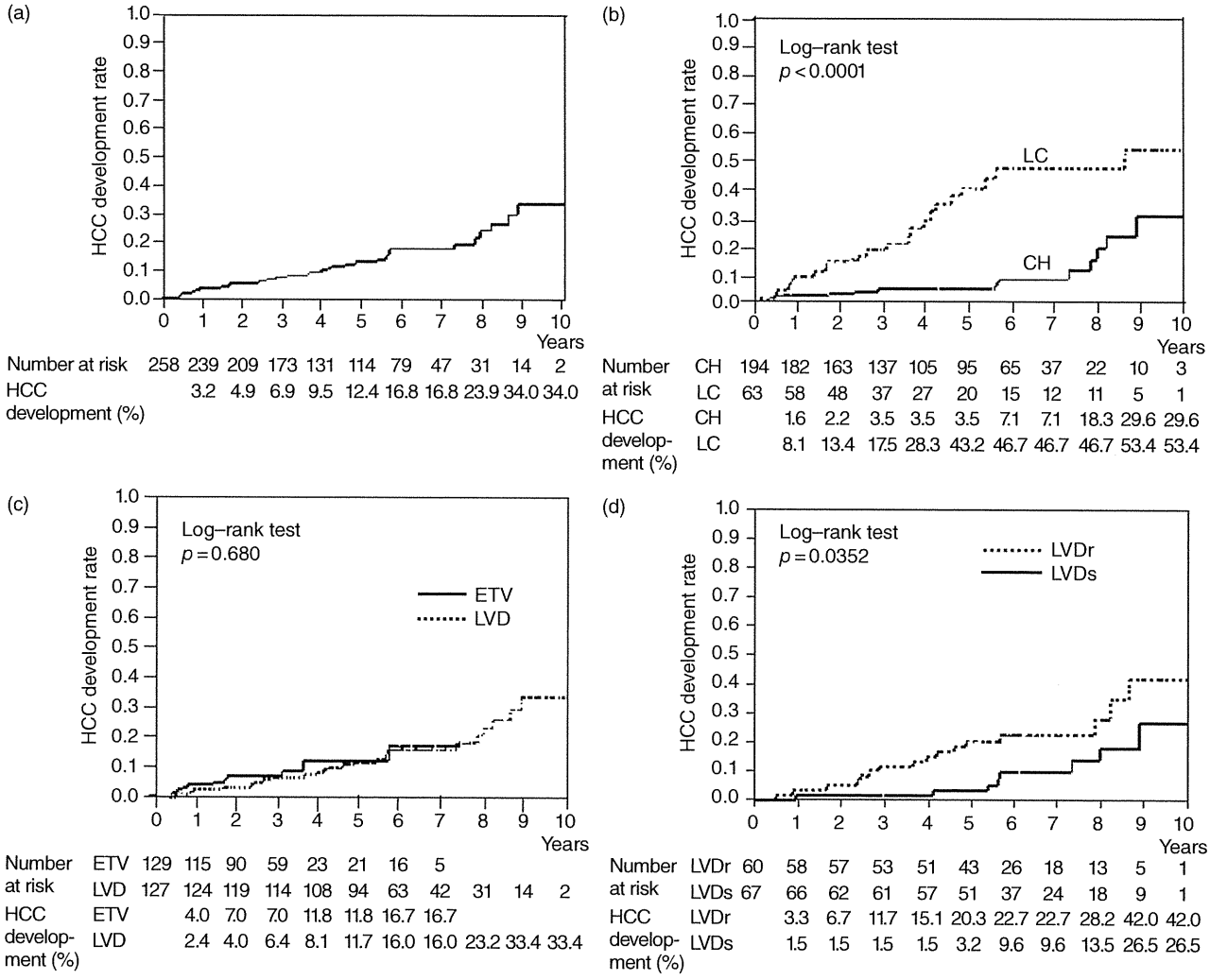

Figure 3 Kaplan–Meier analysis of the incidence of hepatocellular carcinoma (HCC) development with comparison by log–rank test. (a) The cumulative incidence of HCC development at years 1, 3, 5, 7 and 10 in the all patients was 3.2%, 6.9%, 12.4%, 16.8% and 34.0%, respectively. (b) The cumulative incidence of HCC development at years 1, 3, 5, 7 and 10 was 1.6%, 3.5%, 3.5%, 7.1% and 29.6% in chronic hepatitis (CH) patients, and was 8.1%, 17.5%, 43.2%, 46.7% and 53.4% in liver cirrhosis (LC) patients, respectively, with significantly higher incidence in LC than CH patients by log–rank test ($P < 0.0001$). (c) There was no significant difference between the cumulative incidence of HCC between the entecavir (ETV) and lamivudine (LVD) groups by log–rank test ($P = 0.680$). (d) The cumulative incidence of HCC development at years 1, 3, 5, 7 and 10 was 3.3%, 11.7%, 20.3%, 22.7% and 42.0%, respectively, in the patients who developed LVD resistance. It was significantly ($P = 0.0352$) higher as compared with that in patients without LVD resistance, namely, 1.5%, 1.5%, 3.2%, 9.6% and 27.3%, respectively. LVDr, lamivudine resistant; LVDs, lamivudine sensitive.

conclude that NA induced an improvement in the long-term outcome of CHB and cirrhosis patients.

As for drug resistance, LVD resistance cumulatively developed in 60 of 127 patients after a median follow up of 4.25 years, while ETV resistance developed in only one of 129. It was clearly shown that ETV should be selected as the first-line NA for NA-naive patients, as recommended by recent treatment guidelines.[15–18] In patients with LVD resistance, however, co-administration with ADV rescued the antiviral and biochemical effects, and improved hepatic reservation to the same levels as in the ETV group.

The most serious complication of HBV infection is HCC. The annual incidence of HCC from HBV carriers

Table 3 Sensitivity and specificity of AFP and DCP for HCC

Cut-off value	At diagnosis of HCC and at the latest visit						At baseline
	Sensitivity (%)					Specificity (%)	Specificity (%)
	All (n = 35)	Stage 1 (n = 15)	Stage 2 (n = 14)	Stage 3 (n = 5)	Stage 4A (n = 1)		
AFP							
10 ng/mL	45.7	47.0	57.1	20.0	0	97.3	64.4
40 ng/mL	25.7	40.0	28.6	0	0	100	84.6
100 ng/mL	14.3	13.3	21.4	0	0	100	92.0
DCP							
28 mAU/mL	51.5	60.0	50.0	0	100	90.6	82.7
40 mAU/mL	33.3	33.3	35.7	0	100	96.2	95.1
AFP >10 ng/mL and/or DCP >40 mAU/mL	64.7	66.0	71.4	20.0	100	93.4	74.5

AFP, α-fetoprotein; DCP, des-γ-carboxy prothrombin; HCC, hepatocellular carcinoma.

has been reported to be 1% and 3% in patients with CH and cirrhosis, respectively.[20] There are three ways to prevent death from HBV-related HCC: decreasing the risk factors of HCC development, early detection of HCC and a curative treatment. The risk factors include high serum HBV DNA, positive HBeAg, genotype C, precore and core promoter mutations, high ALT levels, cirrhosis, male sex, aging, alcohol, aflatoxin and possibly some single nucleotide polymorphisms.[4,21–25] In these factors, it has been shown that the most important risk is a high serum HBV DNA level.[14] From this point of view, NA treatment, which suppresses HBV replication potently and durably, is naturally expected to suppress hepatocarcinogenesis.[26]

Although interferon has been reported to reduce the incidence of HCC development,[27–29] there have been only a few prospective studies on the effect of NA treatment for suppression of HBV-related HCC development, so far.[12]

In the present prospective study, the cumulative incidence of HCC development at years 1, 3, 5, 7 and 10 after NA treatment was 1.6%, 3.5%, 3.5%, 7.1% and

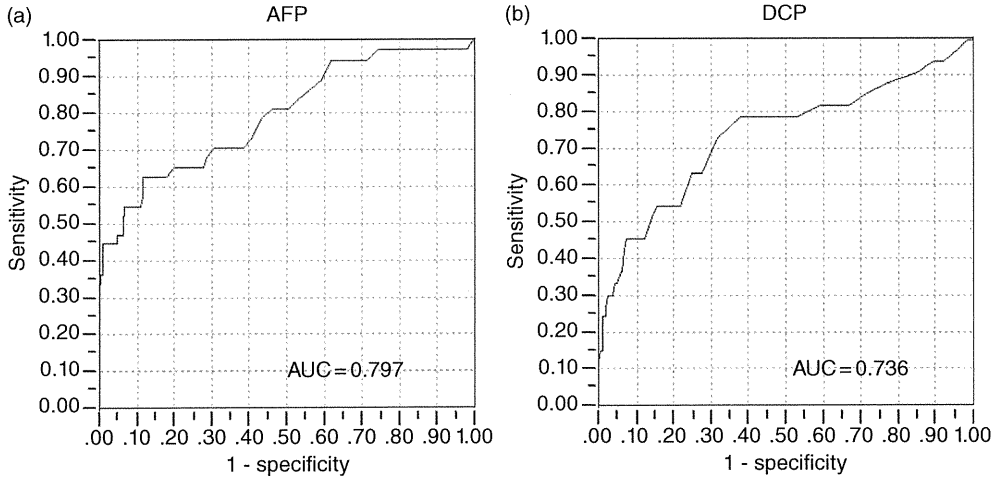

Figure 4 Receiver–operator curve, a plot of sensitivity versus (1 – specificity) over the entire range of the test results was analyzed in search for the optimal cut-off value to distinguish hepatocellular carcinoma (HCC) and non-HCC. (a) The area under the curve (AUC) of α-fetoprotein (AFP) was 0.797. The optimal cut-off value of AFP was approximately 10 ng/mL. (b) The AUC of des-γ-carboxy prothrombin (DCP) was 0.736. The optimal cut-off value of DCP was approximately 40 mAU/mL.

29.6% in CH, and 8.1%, 17.5%, 43.2%, 46.7% and 53.4% in cirrhosis patients, respectively, and there was no difference between ETV and LVD groups. The cumulative incidence of HCC development was almost equivalent to, or somewhat higher than, the conventional reports. In this study, the patient eligibility for enrollment included serum HBV DNA greater than 5 log copies/mL, an elevated ALT level over twice the ULN, or complications of hepatic insufficiency. In other words, we estimated that CHB and cirrhosis patients would have somewhat higher activities or be at more advanced stages. This might be a reason for a higher incidence of HCC development in this study. A direct comparison between patients with and without NA treatment might be necessary for an accurate estimation of the impact of NA on hepatocarcinogenesis. However, such a controlled trial could not be performed due to ethical reasons. Thus, it was a limit of this study that the impact of NA on hepatocarcinogenesis could not be directly estimated.

The majority of the patients who developed HCC, 29 out of 35 cases, were detected at stage 1 or 2. It seemed that scheduled surveillance enabled early detection of HCC, as previously reported,[30] and radical and curative treatments could be performed in 33 out of 35 patients owing to improved hepatic reservation by NA treatment.

Most recent guidelines for HCC screening recommend surveillance every 6 months using US and AFP.[31] The guideline of Japan recommended US screening every 6 months for CH, and every 3 months for cirrhosis, with AFP, AFP-L3 and DCP measurement.[32] Although US is superior to AFP in both sensitivity and specificity for detecting HCC,[31] detection of small HCC by US is frequently difficult because of a very rough parenchymal US-appearance called "mesh-like" in HBV-cirrhosis. In such cases, an elevated AFP level, a continuously elevating AFP in particular, may suggest the development of HCC. Thus, AFP should be employed in combination with imaging.[15]

The sensitivity and specificity of AFP for diagnosis of HCC is insufficient, as previously reported.[33] The sensitivity of AFP for diagnosis of HCC is reported to be approximately 60% at a cut-off of 20 ng/mL,[34,35] and 22–29% at a cut-off of 200 ng/mL.[35,36] The specificity of AFP is reported to be approximately 81–91%[34,35] at a cut-off of 20 ng/mL. AFP may be frequently pseudopositive in CH and cirrhosis. In some guidelines, AFP levels of 100, 200 or 400 ng/mL are offered as cut-off values to elevate specificity.[37]

The present study, however, showed a comparatively high (45.7%) sensitivity of AFP, considering the high ratio of HCC at stage 1 and 2, after NA treatment, at a cut-off value of 10 ng/mL. It is noteworthy that the specificity of AFP, at the cut-off value of 10 ng/mL, became remarkably elevated to 97.3% after NA treatment, although it was merely 64.4% at baseline.

Therefore, the cut-off value of AFP should be lowered to 10 ng/mL in patients receiving NA. The significance of lowering the cut-off level, while maintaining a high specificity, is that it leads to early detection of HCC. A minimal elevation of AFP over 10 ng/mL can result in a high rate of prediction of the development of HCC in NA-treated patients. A similar result has been reported elsewhere.[38]

The sensitivity and specificity of DCP for diagnosis of small HCC, at a cut-off value of 40 mAU/mL, have been reported to be 37–41% and 87–97%, respectively.[35,39–41] In the present study, the sensitivity and specificity of DCP at a cut-off value of 40 mAU/mL was 33.3% and 96.2%, respectively. There was no significant difference in the specificity of DCP, unlike AFP, between baseline and after NA treatment. The combination of AFP and DCP provided a sensitivity of 64.7% and specificity of 93.4%. A recent consensus by the Japan Society of Hepatology recommended a combination of AFP and DCP in high-risk patients.[42]

Recently, it has been speculated that elevated AFP itself is an independent risk factor for HCC. Some reports have shown that AFP can promote the growth of HCC cells.[43–45] In addition, a high AFP level has been correlated with more aggressive behavior and poor prognosis of HCC patients.[46,47] Therefore, a high level of serum AFP can be considered to contribute to the development of HCC rather than merely serving as a tumor marker. Although it remains controversial whether a decrease of AFP could directly reduce the risk and incidence of HCC or not, suppression of AFP production by NA treatment may possibly lead to a reduction in the cellular potential for hepatocarcinogenesis.

In conclusion, the present study demonstrated that long-term NA treatment for CHB and cirrhosis leads to a sustained virological and biochemical effect and improvement of hepatic reservation. Although the impact of NA on hepatocarcinogenesis remained undetermined, it was shown that early detection of HCC was possible by a scheduled surveillance program, and curative treatment could be performed owing to early detection and restored hepatic reservation. The serum AFP level was significantly reduced to lower than 10 ng/mL by NA treatment, resulting in marked elevation of specificity. In NA-treated patients with CHB and cirrhosis, the cut-off value of AFP for HCC surveillance should be

lowered to 10 ng/mL. It is important to note that a minimal elevation of AFP to over 10 ng/mL results in highly accurate prediction of HCC development, leading to earlier detection.

REFERENCES

1 Lavanchy D. Hepatitis B virus epidemiology, disease burden, treatment, and current and emerging prevention and control measures. *J Viral Hepat* 2004; **11**: 97–107.
2 Merican I, Guan R, Amarapuka D *et al.* Chronic hepatitis B virus infection in Asian countries. *J Gastroenterol Hepatol* 2000; **15**: 1356–61.
3 Liaw YF, Tai DI, Chu CM, Chen TJ. Natural course after the development of cirrhosis in patients with chronic type B hepatitis: a prospective study. *Liver* 1989; **9**: 235–41.
4 Wands JR. Prevention of hepatocellular carcinoma. *N Engl J Med* 2004; **351**: 1567–70.
5 Lai CL, Chien RN, Leung NW *et al.* A one-year trial of lamivudine for chronic hepatitis B. Asia Hepatitis Lamivudine Study Group. *N Engl J Med* 1998; **339**: 61–8.
6 Nishida T, Kobashi H, Fujioka S *et al.* A prospective and comparative cohort study on efficacy and drug resistance during long-term lamivudine treatment for various stages of chronic hepatitis B and cirrhosis. *J Gastroenterol Hepatol* 2008; **23**: 794–803.
7 Hadziyannis SJ, Tassopoulos NC, Heathcote EJ *et al.* Long-term therapy with adefovir dipivoxil for HBeAg-negative chronic hepatitis B for up to 5 years. *Gastroenterology* 2006; **131**: 1743–51.
8 Chang TT, Lai CL, Kew Yoon S *et al.* Entecavir treatment for up to 5 years in patients with hepatitis B e antigen-positive chronic hepatitis B. *Hepatology* 2010; **51**: 422–30.
9 Kobashi H, Takaguchi K, Ikeda H *et al.* Efficacy and safety of entecavir in nucleoside-naive, chronic hepatitis B patients: Phase II clinical study in Japan. *J Gastroenterol Hepatol* 2009; **24**: 262–9.
10 Yokosuka O, Takaguchi K, Fujioka S *et al.* Long-term use of entecavir in nucleoside-naïve Japanese patients with chronic hepatitis B infection. *J Hepatol* 2010; **52**: 791–9.
11 Karino Y, Toyota J, Kumada H *et al.* Efficacy and resistance of entecavir following 3 years of treatment of Japanese patients with lamivudine-refractory chronic hepatitis B. *Hepatol Int* 2009; **3**: 403–10.
12 Liaw YF, Sung JJ, Chow WC *et al.* Lamivudine for patients with chronic hepatitis B and advanced liver disease. *N Engl J Med* 2004; **351**: 1521–31.
13 Matsumoto A, Tanaka E, Rokuhara A *et al.* Efficacy of lamivudine for preventing hepatocellular carcinoma in chronic hepatitis B: a multicenter retrospective study of 2795 patients. *Hepatol Res* 2005; **32**: 173–84.
14 Chen CJ, Yang HI, Su J *et al.* Risk of hepatocellular carcinoma across abiological gradient of serum hepatitis B virus DNA level. *JAMA* 2006; **295**: 65–73.
15 Lok ASF, McMahon BJ. Chronic hepatitis B. *Hepatology* 2007; **45**: 507–39.
16 European Association for the Study of the Liver. EASL clinical practice guidelines: management of chronic hepatitis B. *J Hepatol* 2009; **50**: 227–42.
17 Liaw YF, Leung N, Kao JH *et al.* Asian-Pacific consensus statement on the management of chronic hepatitis B: a 2008 update. *Hepatol Int* 2008; **2**: 263–83.
18 Keeffe EB, Dieterich DT, Han SH *et al.* A treatment algorithm for the management of chronic hepatitis B virus infection in the United States: 2008 update. *Clin Gastroenterol Hepatol* 2008; **6**: 1315–41.
19 Liver Cancer Study Group of Japan. *General Rules for the Clinical and Pathological Study of Primary Liver Cancer*, Third English edition. Tokyo: Kanehara & Co.Ltd, 2010.
20 Fattovich G. Natural history of hepatitis B. *J Hepatol* 2003; **39**: S50–8.
21 Chan HL, Hui AY, Wong ML *et al.* Genotype C hepatitis B virus infection is associated with an increased risk of hepatocellular carcinoma. *Gut* 2004; **53**: 1494–8.
22 Kao JH, Chen PJ, Lai MY, Chen DS. Basal core promoter mutations of hepatitis B virus increase the risk of hepatocellular carcinoma in hepatitis B carriers. *Gastroenterology* 2003; **124**: 327–34.
23 Sherman M. Hepatocellular carcinoma: epidemiology, risk factors, and screening. *Semin Liver Dis* 2005; **25**: 143–54.
24 Yuen MF, Yuan HJ, Wong DK *et al.* Prognostic determinants for chronic hepatitis B in Asians: therapeutic implications. *Gut* 2005; **54**: 1610–14.
25 Zhang H, Zhai Y, Hu Z *et al.* Genome-wide association study identifies 1p36.22 as a new susceptibility locus for hepatocellular carcinoma in chronic hepatitis B virus carriers. *Nat Genet* 2010; **42**: 755–8.
26 Lok ASF. Prevention of hepatitis B virus–related hepatocellular carcinoma. *Gastrpenterology* 2004; **127**: S303–9.
27 Niederau C, Heintges T, Lange S *et al.* Long-term follow-up of HBeAg-positive patients treated with interferonalpha for chronic hepatitis B. *N Engl J Med* 1996; **334**: 1422–7.
28 Ikeda K, Saitoh S, Suzuki Y *et al.* Interferon decreases hepatocellular carcinogenesis in patients with cirrhosis caused by the hepatitis B virus: a pilot study. *Cancer* 1998; **82**: 827–35.
29 Lin SM, Sheen IS, Chien RN, Chu CM, Liaw YF. Long-term beneficial effect of interferon therapy in patients with chronic hepatitis B virus infection. *Hepatology* 1999; **29**: 971–5.
30 Zhang BH, Yang BH, Tang ZY. Randomized controlled trial of screening for hepatocellular carcinoma. *J Cancer Res Clin Oncol* 2004; **130**: 417–22.
31 Bruix J, Sherman M. Management of hepatocellular carcinoma. *Hepatology* 2005; **42**: 1208–36.
32 Makuuchi M, Kokudo N, Arii S *et al.* Development of evidence-based clinical guidelines for the diagnosis and treatment of hepatocellular carcinoma in Japan. *Hepatol Res* 2008; **38**: 37–51.

33 Taketa K. Alpha-fetoprotein:Reevaluation in hepatology. *Hepatology* 1990; **12**: 1420–32.
34 Sherman M, Peltekian KM, Lee C. Screening for hepatocellular carcinoma in chronic carriers of hepatitis B virus: incidence and prevalence of hepatocellular carcinoma in a North American urban population. *Hepatology* 1995; **22**: 432–8.
35 Lok AS, Sterling RK, Everhart JE *et al.* Des-gamma-carboxy prothrombin and alpha-fetoprotein as biomarkers for the early detection of hepatocellular carcinoma. *Gastroenterology* 2010; **138**: 493–502.
36 Kai I, Arii S, Okazaki M *et al.* Report of the 17th Nationwide Follow-up Survey of Primary Liver Cancer in Japan. *Hepatol Res* 2007; **37**; 676–91.
37 Bruix J, Sherman M, Llovet JM *et al.* Clinical management of hepatocellular carcinoma. Conclusions of the Barcelona-2000 EASL Conference. *J Hepatol* 2001; **35**: 421–30.
38 Luo K, Liu Z, Karayiannis P. Effect of antiviral treatment on alpha-fetoprotein levels in HBV-related cirrhotic patients: early detection of hepatocellular carcinoma. *J Viral Hepat* 2010; **17**: 511–17.
39 Tsai SL, Huang GT, Yang PM, Sheu JC, Sung JL, Chen DS. Plasma des-gamma-carboxyprothrombin in the early stage of hepatocellular carcinoma. *Hepatology* 1990; **11**: 481–8.
40 Cui R, Wang B, Ding H, Shen H, Li Y, Chen X. Usefulness of determining a protein induced by vitamin K absence in detection of hepatocellular carcinoma. *Chin Med J (Engl)* 2002; **115**: 42–5.
41 Nakamura S, Nouso K, Sakaguchi K *et al.* Sensitivity and specificity of des-gamma-carboxy prothrombin for diagnosis of patients with hepatocellular carcinomas varies according to tumor size. *Am J Gastroenterol* 2006; **101**: 2038–43.
42 Arii S, Sata M, Sakamoto M *et al.* Management of hepatocellular carcinoma: report of consensus meeting in the 45th Annual Meeting of the Japan Society of Hepatology (2009). *Hepatol Res* 2010; **40**: 667–85.
43 Wang XW, Xie H. Alpha-fetoprotein enhances the proliferation of human hepatoma cells in vitro. *Life Sci* 1999; **64**: 17–23.
44 Li MS, Li PF, He SP, Du GG, Li G. The promoting molecular mechanism of alpha-fetoprotein on the growth of human hepatoma Bel7402 cell line. *World J Gastroenterol* 2002; **8**: 469–75.
45 Li MS, Li PF, Chen Q, Du GG, Li G. Alpha-fetoprotein stimulated the expression of some oncogenes in human hepatocellular carcinoma Bel 7402 cells. *World J Gastroenterol* 2004; **10**: 819–24.
46 Peng SY, Chen WJ, Lai PL, Jeng YM, Sheu JC, Hsu HC. High alpha-fetoprotein level correlates with high stage, early recurrence and poor prognosis of hepatocellular carcinoma: significance of hepatitis virus infection, age, p53 and betacatenin mutations. *Int J Cancer* 2004; **112**: 44–50.
47 Zhou YM, Yang JM, Li B *et al.* Risk factors for early recurrence of small hepatocellular carcinoma after curative resection. *Hepatobiliary Pancreat Dis Int* 2010; **9**: 33–7.

Nakanishi et al. BMC Cancer 2011, 11:3
http://www.biomedcentral.com/1471-2407/11/3

BMC Cancer

RESEARCH ARTICLE Open Access

Loss of runt-related transcription factor 3 expression leads hepatocellular carcinoma cells to escape apoptosis

Yutaka Nakanishi[1], Hidenori Shiraha[1*], Shin-ichi Nishina[1], Shigetomi Tanaka[1], Minoru Matsubara[1], Shigeru Horiguchi[1], Masaya Iwamuro[1], Nobuyuki Takaoka[1], Masayuki Uemura[1], Kenji Kuwaki, Hiroaki Hagihara, Junichi Toshimori, Hideki Ohnishi[1], Akinobu Takaki[1], Shinichiro Nakamura[1], Yoshiyuki Kobayashi[1], Kazuhiro Nouso[1,2], Takahito Yagi[3], Kazuhide Yamamoto[1]

Abstract

Background: Runt-related transcription factor 3 (RUNX3) is known as a tumor suppressor gene for gastric cancer and other cancers, this gene may be involved in the development of hepatocellular carcinoma (HCC).

Methods: RUNX3 expression was analyzed by immunoblot and immunohistochemistry in HCC cells and tissues, respectively. Hep3B cells, lacking endogenous RUNX3, were introduced with RUNX3 constructs. Cell proliferation was measured using the MTT assay and apoptosis was evaluated using DAPI staining. Apoptosis signaling was assessed by immunoblot analysis.

Results: RUNX3 protein expression was frequently inactivated in the HCC cell lines (91%) and tissues (90%). RUNX3 expression inhibited 90 ± 8% of cell growth at 72 h in serum starved Hep3B cells. Forty-eight hour serum starvation-induced apoptosis and the percentage of apoptotic cells reached 31 ± 4% and 4 ± 1% in RUNX3-expressing Hep3B and control cells, respectively. Apoptotic activity was increased by Bim expression and caspase-3 and caspase-9 activation.

Conclusion: RUNX3 expression enhanced serum starvation-induced apoptosis in HCC cell lines. RUNX3 is deleted or weakly expressed in HCC, which leads to tumorigenesis by escaping apoptosis.

Background

Hepatocellular carcinoma (HCC)[1] is the sixth most common cancer and responsible for more than half a million deaths worldwide each year [1-3]. Although most HCC cases occur in East Asia and Middle and West Africa, its incidence in some developed countries is increasing [1,4]. In most cases, HCC is fatal because of an incomplete understanding of the pathogenic mechanisms and inadequacies of early detection [1,5].

The activation of proto-oncogenes plays a major role in the development of HCC [1,6-8], and a number of tumor suppressor genes may be associated with the development and progression of HCC [1,9-12]. Although several cancer-related genes are altered in HCC, the frequency of alterations for each individual gene is relatively low. In HCC, the alteration of tumor suppressor genes seems to be more important than that of oncogenes. Established genetic events include the loss of an allele, mutation, or promoter methylation [13-16]. A higher loss of heterozygosity (LOH) frequency was detected at several loci on chromosomes 8p23, 4q22-24, 4q35, 17p13, 16q23-24, 6q27, 1p36, and 9p12-14, suggesting the presence of important tumor suppressor genes at these loci [17]. However, there is little understanding of the several key pathways and the genes involved in these pathways.

Runt-related transcription factor 3 (RUNX3), located on chromosome 1p36, is correlated with tumorigenesis and gastric cancer progression [18,19]. RUNX3 acts as

* Correspondence: hshiraha@md.okayama-u.ac.jp
[1]Department of Gastroenterology and Hepatology, Okayama University Graduate School of Medicine and Dentistry, 2-5-1 Shikata-cho, Okayama 700-8558, Japan
Full list of author information is available at the end of the article

an apoptotic factor, downstream of transforming growth factor-β (TGF-β), and as a cell differentiation mediator in intestinal metaplasia of gastric mucosa [19-21]. In gastric cancer cell lines, RUNX3-induced apoptosis depends on Bim expression [22]. RUNX3 protein expression is decreased about 45-60% in human gastric cancer [21] and has been detected in some human malignancies such as those of the colon, lung, pancreas, and bile duct [23-26]. RUNX3 gene expression decreased in 30-80% of HCCs due to LOH and methylation of its promoter [27,28]. The loss or decrease of RUNX3 expression in HCC tissue has been recently reported [29], but the precise function of RUNX3 in HCC needs to be elucidated.

Methods

Cell lines and cell culture

The HCC cell lines HepG2, Hep3B, PLC/PRF/5 (PLC), and SK-Hep1 were obtained from the American Type Culture Collection (Manassas, VA), and the Huh1, Huh7, JHH1, JHH2, JHH4, HLE, and HLF cell lines were obtained from the Health Science Research Resources Bank (Osaka, Japan). Normal human hepatocytes were obtained from Sanko Junyaku Co. Ltd. (Tokyo, Japan). JHH2 and normal human hepatocytes were cultured in William's medium E (Invitrogen, Carlsbad, CA). Other cell lines were maintained in Dulbecco's modified Eagle's medium (Invitrogen). Media were supplemented with 10% heat-inactivated fetal bovine serum (FBS) (Sigma, St. Louis, MO), 1% nonessential amino acids (Sigma), 1% sodium pyruvate (Sigma), and 1% penicillin/streptomycin solution (Sigma). Cells were cultured at 37°C in a humidified atmosphere of 5% CO_2 and 95% air. Quiescence was carried out under restricted serum conditions with 0.1% dialyzed FBS for the indicated time periods.

RNA preparation and reverse transcriptase-polymerase chain reaction

Total RNA was isolated from cells using Trizol™ reagent (Invitrogen). Reverse transcription was performed using random primers and ReverTra Ace™ (Toyobo, Osaka, Japan) reverse transcriptase (RT). Ps-CA and Ps-CB, previously published primer set for RUNX3, were utilized [21]. For each polymerase chain reaction (PCR), 20 μl (total volume) of reaction mixture contained 0.1 μg template DNA, 4 pmol each of the forward and reverse primers, 2 μl deoxynucleoside triphosphates (200 mM each), 1 U pfu Turbo™ DNA polymerase (Stratagene, La Jolla, CA), and 2 μl of 10× pfu reaction buffer. PCR amplification was conducted on an iCycler™ (Bio-Rad, Hercules, CA) with the following cycle conditions: cycle 1, 95°C for 2 min; cycles 2-30, 95°C for 30 s, 58°C for 30 s, and 72°C for 120 s, with a final elongation step of 72°C for 10 min.

Immunoblot analysis

Cells were plated onto 6-well tissue culture plastic dishes and grown to confluence. After cultivating the cells under the indicated conditions, they were washed twice with cold phosphate-buffered saline (PBS) and lysed in 150 μl of sample buffer (100 mM Tris-HCl, pH 6.8, 10% glycerol, 4% sodium dodecyl sulfate [SDS], 1% bromophenol blue, 10% β-mercaptoethanol). The samples were resolved by SDS-polyacrylamide gel electrophoresis (PAGE) and transferred to Immobilon-P™ polyvinylidene difluoride membranes (Millipore Corporation, Bedford, MA), which were blocked using Tris-buffered saline with Tween-20 (TBS-T) (Sigma) containing 5% bovine serum albumin for 1 h. The membranes were incubated with antibodies against RUNX3 (R3-G54; Abcam, Cambridge, MA), poly-histidine (His) (Roche Diagnostics, Basel, Switzerland), Bax, Bcl-2, Bim, cleaved caspase-3 and -9 (Cell Signaling Technology, Beverley, MA), and β-actin (Sigma) overnight at 4°C. We washed the membranes three times with TBS-T and probed with horseradish peroxidase-conjugated secondary antibodies before developing them using an ECL Western blotting detection system (Amersham Biosciences, Piscataway, NJ) by enhanced chemiluminescence.

HCC tissue and immunohistochemistry

Thirty-one patients including 24 men with age ranging from 18 to 71 years (average age, 58 years) and 7 women with age ranging from 59 to 67 years (average age, 63 years) at the time of hepatic resection were included in this study. HCC tissues along with adjacent liver tissues were used for analysis. As per the institutional guidelines, we obtained informed consent from all donors of liver tissue samples, and the study was approved by the Research Ethics Committee of Okayama University.

Immunohistochemistry was performed on formalin-fixed paraffin sections that were dewaxed and dehydrated. After rehydration, endogenous peroxidase activity was blocked for 30 min in a methanol solution containing 0.3% hydrogen peroxide. After antigen retrieval in citrate buffer, the sections were blocked overnight at 4°C. The sections were probed with rabbit polyclonal antibody (ab49117; Abcam) followed by biotinylated anti-rabbit secondary antibody (Dako Japan, Tokyo, Japan). The signal was amplified by avidin-biotin complex formation and developed with diaminobenzidine followed by counterstaining with hematoxylin, after which the sections were dehydrated in alcohol and xylene, and mounted for observation. The sections were scored on a four-tier scale; 0, negative; 1, weak signal; 2, intermediate signal; and 3, strong signal [30]. All sections were scored independently by two observers (Y. K. and K. N.) without prior knowledge. All discrepancies in scoring were reviewed and a consensus was reached.

RUNX3 cloning and transfection

We obtained human RUNX3 cDNA by PCR-based cloning from normal human hepatocytes (Sanko Junyaku). Briefly, cDNA was amplified by PCR using sense (5'-TATGCGTATTCCCGTAGA) and antisense (5'-CTCGAGGCGGCCGCTCAATGGTGATGGTGATGATGACCGGTACGGTAGGGCCGCCACAC; including the six-His tag) oligonucleotide primers with Pfu Turbo™ Hotstart DNA polymerase (Stratagene) and cloned into the PCR II TA cloning vector (Invitrogen). The size of the PCR product was ~1.2 kb. After confirmation by sequencing, RUNX3 cDNA was subcloned into pCEP4 (Stratagene), downstream from a cytomegalovirus promoter. The poly-His tag was replaced with green fluorescent protein (GFP) cDNA from pEGFP-C1 (Clontech, Palo Alto, CA). The human RUNX3 and/or chloramphenicol acetyltransferase (CAT) (control) constructs were transfected into Hep3B cells using FuGENE™6 transfection reagent (Roche), as per the manufacturer's instruction. Cells were selected in complete medium containing 250 μg/ml of hygromycin (Roche). Polyclonal lines consisting of more than 20 colonies were established. At least two independent stably transfected lines were established for each construct.

Transient RUNX3 expression was also conducted using FuGENE™6 in Hep3B, Huh7, HLE, and HLF cells. After transfection, the cells were cultured under serum starved condition for the indicated periods, if needed, and utilized for the following experiments.

MTT assay

Cell proliferative activity was assessed with the 3-(4, 5-dimethylthiazol-2-yl)-2, 5-diphenyl tetrazolium bromide (MTT) assay. Briefly, cells were seeded at 2,000 cells/well in 96-well tissue culture plastic dishes and quiesced for 6 h with 0.1% dialyzed FBS. After 24-120 h of quiescence, the cells were cultured for the indicated periods with or without 10% FBS. At the end of the treatment, 10 μl of MTT (5 mg/ml in PBS) was added to each well, and the wells were incubated for an additional 2 h at 37°C. The purple-blue MTT formazan precipitate was dissolved in 200 μl of dimethyl sulfoxide (Sigma). The activity of the mitochondria, reflecting cellular growth and viability, was evaluated by measuring the optical density at 570 nm with a microplate reader (Bio-Rad).

DAPI staining

Cells were plated at 50% confluence on glass chamber slides (Labtek II, Nalgen Nunc, Roskide, Denmark) and quiesced for 6 h with a media containing 0.1% dialyzed FBS. Then, they were treated with 10% FBS, 100 μM caspase inhibitor (caspase inhibitor IV, Calbiochem, Gibbstown, NJ), 1 nM transforming growth factor-α (TGF-α) (Peprotech Inc. Rocky Hill, NJ), 1 nM epidermal growth factor (EGF) (Peprotech), and/or 5 ng/ml platelet derived growth factor (PDGF)-BB (Peprotech). Chromosomal DNA was stained with 4', 6-diamidine-2'-phenylindole dihydrochloride (DAPI) (Dojindo, Kumamoto, Japan) according to the manufacturer's instructions. Briefly, treated cells were washed with PBS and stained with DAPI working solution (1 μg/ml in PBS) for 2 min. The percentage of cells with condensed chromatin and/or fragmented nuclei was established in 300-500 DAPI-stained cells examined under a fluorescence microscope (IX-70, Olympus, Tokyo, Japan).

Flow cytometry analysis

Annexin V and propidium iodide (PI) staining was performed using an annexin V-fluorescein isothiocyanate (FITC) Apoptosis Detection kit (Medical & Biological Laboratories Co., Ltd., Nagoya, Japan) to measure apoptosis. Cells were cultured in 10-cm tissue culture plates and quiesced for 6 h with a media containing 0.1% dialyzed FBS. Cells were cultured in medium with or without 10% FBS for 24 h. Then, they were washed twice with PBS, collected, and re-suspended in 85 μl of 1× annexin V-FITC binding buffer. Five microliters of annexin V-FITC conjugate and 10 ml of PI buffer were added, and the cells were incubated at room temperature for 15 min in the dark. After adding 400 μl of 1× annexin V-FITC binding buffer, cells were analyzed using a flow cytometer (FACS Calibur; Becton Dickinson, Franklin Lakes, NJ).

Gene silencing of Bim with small interfering RNA

RUNX3-expressing Hep3B cells were transfected with either scrambled negative control small interfering RNA (siRNA) or Bim siRNA (Applied Biosystems, Foster City, CA). siRNAs were transfected into cells using RNAi-Fect™ transfection reagent (Qiagen, Hilden, Germany). Cells were incubated with scrambled negative control siRNA or Bim siRNA for 24 h before 48 h of serum starvation. The MTT assay and DAPI staining for detecting apoptosis were performed as described above.

Results

Loss of RUNX3 expression in HCC cell lines and human HCC tissues

A decreased level or absence of RUNX3 mRNA expression was observed in 10 of 11 HCC cell lines (Figure 1A). RUNX3 mRNA was undetectable in eight cell lines (HepG2, Hep3B, Huh1, Huh7, JHH1, JHH2, JHH4, and HLE). In HLF and SK-Hep1 cells, RUNX3 mRNA was significantly underexpressed (Figure 1A). Normal human hepatocytes expressed RUNX3 mRNA. Sequence analysis was performed in HLF, PLC, and SK-Hep1 cells, and no mutation was detected. In accordance with the mRNA analysis, RUNX3 protein expression was

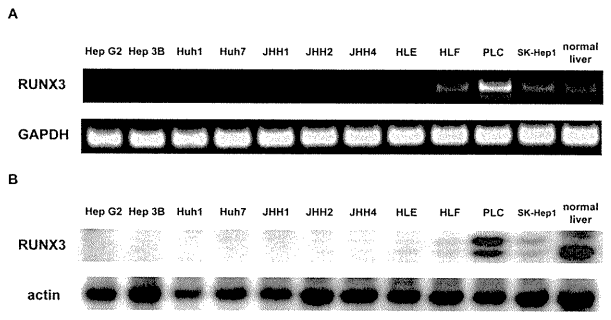

Figure 1 RUNX3 mRNA (A) and protein (B) expression in HCC cell lines. (A) RUNX3 and GAPDH mRNA expression levels were determined by RT-PCR. Shown here are representative gels from three independent experiments. (B) RUNX3 and α-actin protein expression was analyzed by immunoblot using the anti-RUNX3 antibody. Shown here are representative blots from more than three independent experiments.

undetectable in the HepG2, Hep3B, JHH1, JHH2, JHH4, HLE, and HLF cell lines, while the RUNX3 protein was expressed in HLF, PLC, and SK-Hep1 cells (Figure 1B). The RUNX3 protein was significantly underexpressed in HLF and SK-Hep1 cells.

RUNX3 protein expression in human HCC tissue was compared to that in the corresponding tumor-free resection margins using immunohistochemical analysis (Figure 2). Twenty eight (~90%) of these pairs showed a negative or weak signal for RUNX3 expression in HCC tissue, but showed RUNX3 protein expression in tumor-free resection margins (Table 1). In the remaining three pairs, a weak RUNX3 expression signal was detected in the tumor-free resection margins; thus, no negative RUNX3 signal was detected in the tumor-free resection margins.

Ectopic RUNX3 protein expression in Hep3B cells

To assess whether RUNX3 protein expression affected cell survival in the HCC cell lines, a RUNX3 construct was introduced into RUNX3-negative Hep3B cells (Figure 3A). Overall, the clones were expressed at similar

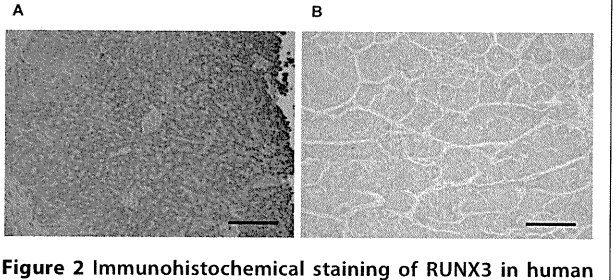

Figure 2 Immunohistochemical staining of RUNX3 in human liver tissues. (A) nontumor liver tissue with a protein score of 3 (B) HCC tissue with a protein score of 0. Bar = 100 μm.

Table 1 RUNX3 expression in HCC samples (n = 31) and the corresponding tumor-free resection margins

RUNX3 protein expression score	HCC samples (n = 31)	Tumor-free sections (n = 31)
0 (negative signal)	13 (41.9%)	0
1 (weak signal)	15 (48.4%)	3 (9.7%)
2 (intermediate signal)	3 (9.7%)	16 (51.6%)
3 (strong signal)	0	12 (38.7%)

levels in all cells, as determined by immunocytochemical analysis (data not shown). RUNX3-expressing Hep3B cells grew slightly slower than normal Hep3B cells in the presence of FBS.

RUNX3 expression inhibited cell growth under serum starvation

RUNX3 has been reported to induce apoptosis in a gastric cancer cell study [21]. The MTT assay was performed to determine whether RUNX3 expression influenced cell growth. RUNX3-expressing Hep3B cells grew slightly slower than CAT-transfected Hep3B cells in the presence of FBS, whereas the growth of RUNX3-expressing Hep3B cells was markedly suppressed in the absence of FBS; growth inhibition could be observed as early as 24 h, and reached 70 ± 12% and 90 ± 8% at 48 and 72 h, respectively (Figure 3B). The inhibition levels were over 4 times than those found in the condition with 10% FBS. This effect was confirmed with GFP-tagged RUNX3-expressing Hep3B cells (70 ± 11% growth inhibition at 72 h).

RUNX3 expression induced apoptosis under serum starvation

The effect of RUNX3 expression on cell survival and the cell cycle with and without FBS was assessed to investigate whether the elicited growth suppression in RUNX3-expressing cells under serum starved conditions was due to an increase in cell death or due to cell cycle inhibition, or both. DAPI staining demonstrated that serum starvation induced apoptosis in RUNX3-expressing Hep3B cells (31 ± 4%) but not in CAT-transfected Hep3B cells (4 ± 1%) in the absence of FBS (Figure 3C). Flow cytometry analysis with annexin V antibody was also performed. RUNX3-expressing Hep3B cells showed a significant increase in a pre-apoptosis population (Annexin V+ PI-) after 24 h of serum starvation compared with CAT-transfected Hep3B cells (Figure 3D).

RUNX3-induced apoptosis through the Bim-caspase pathway

Because a RUNX3-induced apoptotic pathway has been described previously, the effect of altering RUNX3 expression was investigated. Bim protein expression was

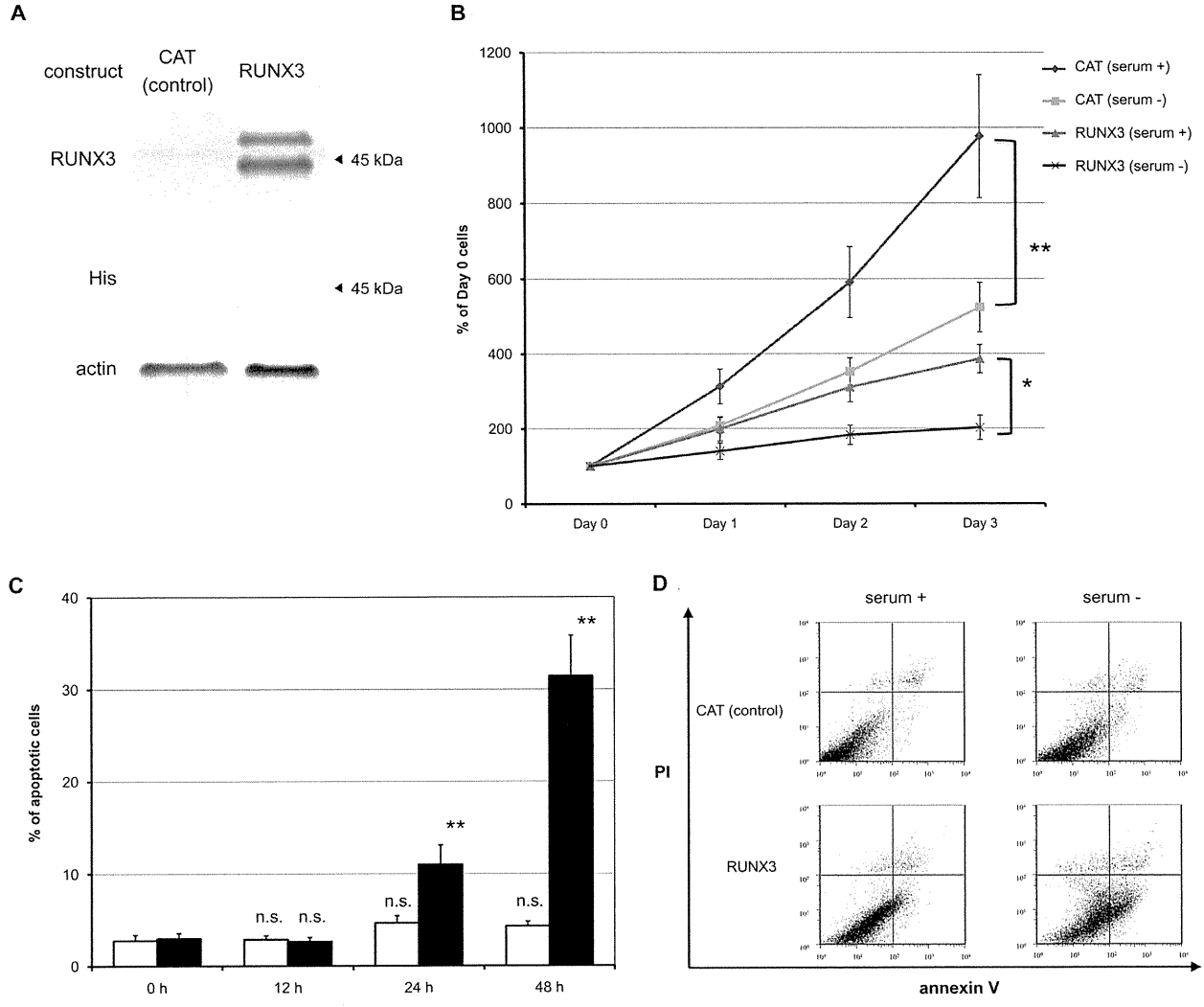

Figure 3 RUNX3 expression in Hep3B cells. CAT (control) and RUNX3 constructs were introduced into Hep3B cells. Polyclonal stably expressing cell lines were selected in the presence of hygromycin. (A) Immunoblot analysis RUNX3 protein expression was analyzed by immunoblot using anti-RUNX3 and anti-His antibodies. Shown here are representative blots from more than three independent experiments. (B) Effect of RUNX3 expression on cell growth Cell proliferative activities were measured by the MTT assay. All results are expressed as ratios to cell number at day 0. Data represent the mean ± S.E. of more than three independent experiments, each with four replicates. *, $P < 0.05$; **, $P < 0.01$ (vs. data at 0 h); Student's *t*-test. (C) Apoptosis determined by DAPI staining Cells were cultured in medium without FBS for the indicated periods. The cells were stained with DAPI, and the percentage of apoptotic cells was examined by fluorescence microscopy (CAT; white bars, RUNX3; black bars). Data represent the mean ± S.E. of more than five independent experiments, each with triplicates. n.s., not significant; **, $P < 0.01$ (vs. data at 0 h); Student's *t*-test. (D) Flow cytometry analysis Cells were cultured in medium with or without 10% FBS for 24 h. They were harvested and washed in PBS without Ca^{2+}/Mg^{2+}, and stained using the Mebcyto™ apoptosis detection kit. The cells were analyzed with a Becton Dickinson FACS Calibur flow cytometer. Shown here are representative plots from more than three independent experiments.

enhanced by serum starvation in RUNX3-expressing Hep3B cells but not in control cells (Figure 4A). Activated apoptosis executors, caspase-9 and -3, were found in serum starved RUNX3-expressing Hep3B cells. Expression of the Bim attenuators, Bax and Bcl-2, was not affected by serum starvation. These results imply that Bim plays a major role in serum starvation-induced apoptosis in RUNX3-expressing cells.

Serum starvation-induced apoptosis was abrogated by an apoptosis inhibitor (Figure 4B). Various growth factors were employed to determine whether serum starvation-induced apoptosis was caused by the absence of a growth factor-induced survival signal. As a result, TGF-α, EGF, and PDGF abrogated serum starvation-induced apoptosis in RUNX3-expressing Hep3B cells (Figure 4B).

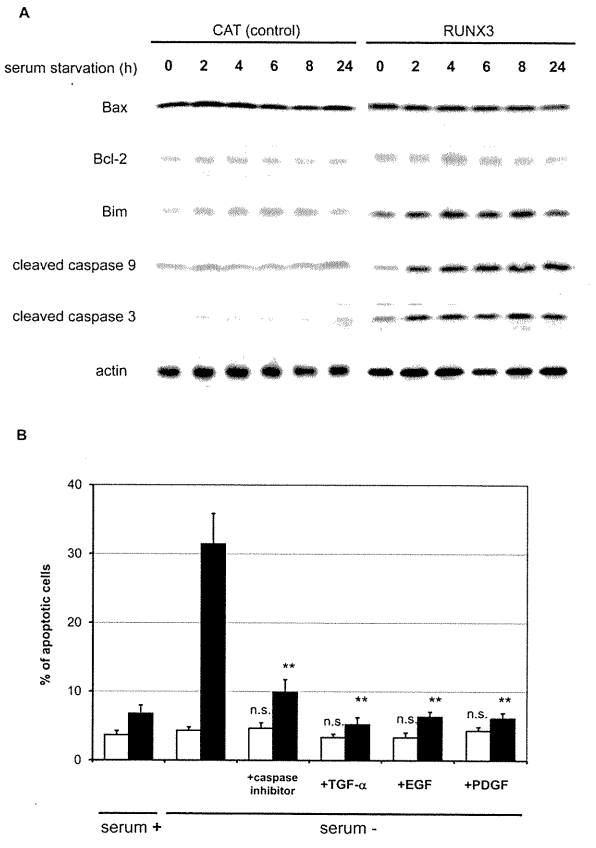

Figure 4 Effect of RUNX3 on apoptosis-related signaling molecules. (A) Immunoblot analysis Equal amounts of cell lysates were size-fractionated with 10% SDS-PAGE and immunoblotted with antibodies against Bax, Bcl-2, Bim, cleaved caspase-9, cleaved caspase-3, and actin. Shown here are representative blots from at least three independent experiments. (B) Apoptosis determined by DAPI staining Cells were cultured in media with or without 10% FBS, caspase inhibitor, and/or TGF-α for 48 h. Cells were stained with DAPI, and the percentage of apoptotic cells was determined under a fluorescent microscope (CAT; white bars, RUNX3; black bars). Data represent the mean ± S.E. of more than five independent experiments, each with triplicates. n.s., not significant; $P > 0.05$; **, $P < 0.01$ (vs. data with no serum); Student's *t*-test.

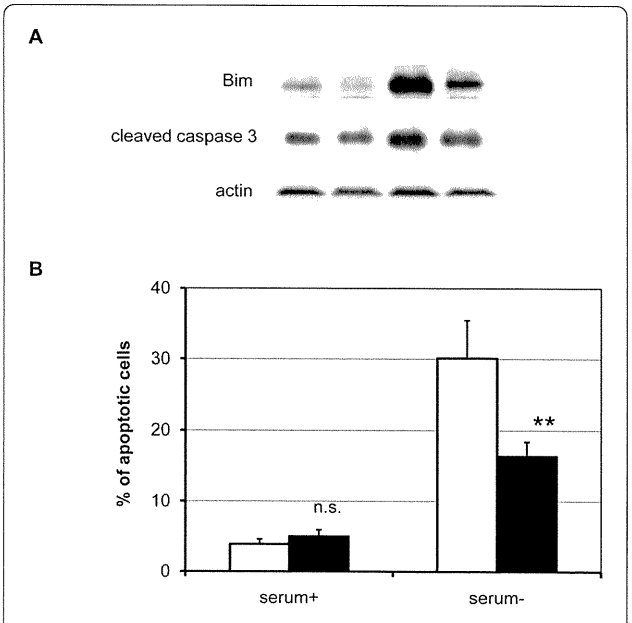

Figure 5 Effect of Bim siRNA gene silencing on cell growth inhibition and apoptosis. After treatment with Bim siRNA duplexes, an immunoblot analysis (A) and DAPI apoptosis detection assay (B) were performed. Shown here are representative blots from more than three independent experiments. All results are expressed as ratios to control siRNA-treated cells (control siRNA, white bars; Bim siRNA, black bars). Data are mean ± S.E. from at least three independent experiments, each performed in triplicate. Statistical analysis was performed with the Student's *t*-test. n.s., not significant; **, $P < 0.01$ (vs. control siRNA-treated cells).

siRNA against Bim reduced serum starvation-induced apoptosis in RUNX3-expressing Hep3B cells

siRNA against Bim was used to knockdown Bim expression in Hep3B cells (Figure 5A). The expression level of cleaved caspase-3, decreased in Bim siRNA-treated cells (Figure 5A). Bim siRNA inhibited serum starvation-induced apoptosis by 46 ± 7% in RUNX3-expressing Hep3B cells (Figure 5B).

Transient ectopic RUNX3 expression in various HCC cell lines

RUNX3 was transiently expressed in various HCC cell lines, including Hep3B, Huh7, HLE, and HLF, introducing a RUNX3 construct-induced RUNX3 protein expression (Figure 6A). Transient RUNX3-expressing cells also showed growth inhibition after 48 h of serum starvation; the inhibition was 50 ± 10%, 46 ± 11%, 60 ± 8%, and 52 ± 9% in Hep3B, Huh7, HLE, and HLF cells, respectively. The RUNX3-expressing HCC cell lines demonstrated enhanced serum starvation-induced apoptosis; the percentage of apoptotic cells determined by DAPI staining was 21 ± 2%, 25 ± 2%, 19 ± 1%, and 20 ± 2% in Hep3B, Huh7, HLE, and HLF cells, respectively (Figure 6B). Serum starvation-induced Bim expression and caspase-3 cleavage were also confirmed in RUNX3-expressing Hep3B, Huh7, HLE, and HLF cells (Figure 6C).

Discussion

The results of the present study demonstrated that RUNX3 is a tumor suppressor gene for HCC. A significant down-regulation of RUNX3 was observed in a high percentage of human HCC cell lines (91%) and tissues (90%) (Figures 1, 2, and Table 1). RUNX3 has been described as a gastric cancer tumor suppressor [21]. In many cancer types, deletion of the RUNX3 locus and reduction of its expression by promoter hypermethylation has been

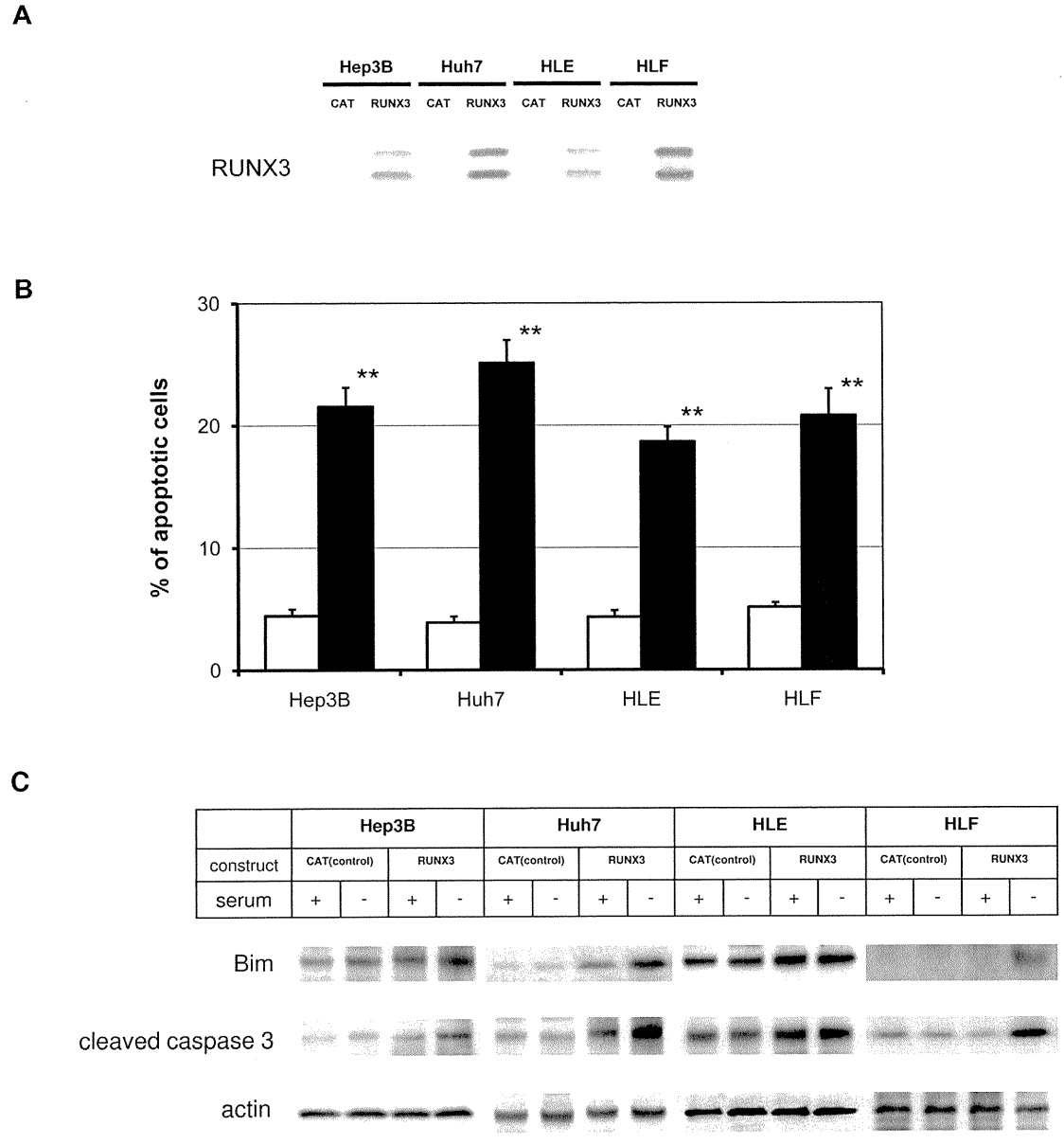

Figure 6 Effect of transient ectopic RUNX3 expression. CAT (control) and RUNX3 constructs were introduced into HCC cell lines. After a 48-h incubation period, an immunoblot analysis for RUNX3 expression (A), a DAPI apoptosis detection assay (B), and an immunoblot analysis for Bim and caspase (C) were performed. Shown here are representative blots from more than three independent experiments. All results are expressed as ratios to control CAT-transfected cells (CAT; white bars, RUNX3; black bars). Data represent the mean ± S.E. of more than five independent experiments, each with triplicates. **, $P < 0.01$ (vs. data at 0 h); Student's *t*-test.

reported [23-26]. However, little is known about the role of RUNX3 in HCC tumor suppression. We hypothesized that loss of RUNX3 expression contributes the development of HCC by escaping apoptosis. The results of the present study provide clear evidence that RUNX3 elicits serum starvation-induced apoptosis in HCC cells by activating the Bim-caspase pathway.

Stable expression of RUNX3 protein was established in Hep3B cells (Figure 3A), and they showed apoptosis under serum starved conditions (Figure 3B). This effect was reproducible in the Hep3B, Huh7, HLE, and HLF HCC cell lines transiently expressing RUNX3. The inhibition of cell growth in transient RUNX3-expressing cells was generally lower than that in stable RUNX3-

expressing Hep3B cells, probably due to low transfection efficiency.

Serum starvation-induced apoptosis is caused by caspase activation in ectopic RUNX3-expressing Hep3B cells (Figures 3C and 3D). To explore the signaling molecule responsible for apoptosis, Bim protein expression was induced in serum starved RUNX3-expressing Hep3B cells (Figure 4A). This is the first report demonstrating that RUNX3 enhances Bim expression under serum starved conditions in HCC cells, which appears to be consistent with the important role of Bim in previous studies on other types of cells. Bim expression was induced by the cooperation of RUNX3 and TGF-β in a study of gastric epithelial cells [21,31]. Bim protein also plays an important role in cell death [32]. Bim induces sequential activation of caspase-9 and -3 [32]. The potency of Bim as a cell death inducer is attenuated by Bax and Bcl-2 subfamily proteins [33]. The expression of Bax and Bcl was not affected by RUNX3 expression (Figure 4A). The expression of Bad (data not shown), a Bcl-2 antagonist known as a serum starvation-induced apoptosis initiator [34], increased with serum starvation but was not attenuated by RUNX3 expression (Figure 4A). Bim siRNA was used to evaluate whether Bim expression regulates serum starvation-induced apoptosis in RUNX3-expressing cells. As a result, Bim siRNA successfully knocked down Bim expression in RUNX3-expressing Hep3B cells (Figure 5A). Knockdown of Bim expression abrogated serum starvation-induced apoptosis in RUNX3-expressing Hep3B cells (Figure 5B). Consequently, RUNX3 expression enhanced serum starvation-induced apoptosis through the Bim-caspase pathway in Hep3B cells. This effect was reproducible in the Huh7, HLE, and HLF HCC cell lines transiently expressing RUNX3 (Figure 6).

Serum starvation triggered apoptosis in RUNX3-expressing HCC cells. As this leads to the question of how serum prevents apoptosis in RUNX3-expressing cells, RUNX3-expressing Hep3B cells were treated with TGF-α, EGF, or PDGF (Figure 4C). These growth factors reduced apoptosis in RUNX3-expressing Hep3B cells by activating the PI3/Akt signaling pathway (data not shown), which is consistent with a previous report [34].

RUNX3 induces apoptosis in the presence of TGF-β [21]. In a study of gastric epithelial cells, RUNX3 enhanced Bim expression during TGF-β-induced apoptosis [21,31]. In a study of a gastric and esophageal cancer cell lines, RUNX3 expression made cancer cells sensitive to TGF-β-induced apoptosis [21,35-38]. These reports suggest that TGF-β is required for RUNX3-related apoptosis. In the present study, ectopic RUNX3 expression enhanced serum starvation-induced apoptosis in the absence of TGF-β. This discrepancy may be explained by the autocrine action of TGF-β in Hep3B cells, which have an intact TGF-β signaling pathway [39]. Furthermore, some HCC cell lines, including Hep3B, produce TGF-β [40]. Further study is required to establish whether TGF-β is involved in the enhanced apoptosis of HCC.

It has been reported that p53, Rb, p16, phosphatase, and tensin homolog (PTEN) are altered in HCC. The p53 gene is the most extensively studied gene of solid tumors. Alteration of this gene occurs at a relative low frequency (28-42%) in HCC compared to other solid tumors [11,17,41,42]. The Rb gene is another well-studied tumor suppressor gene in HCC and other solid tumors. Rb mutations are found in only 15% of HCCs [42]. The LOH of chromosome 13q, where Rb gene is located, is more frequent in HCC (25-48%) [43,44]. The p16 gene, also known as the cyclin-dependent kinase inhibitor 2A gene, regulates the Rb pathway and is found in 64% of HCCs [9]. PTEN negatively regulates the PI3K/Akt signaling pathway, which is involved in the regulation of cell survival [45]. Alteration of PTEN was found in ~40% of HCCs [10]. The frequency of alteration of each individual gene was relatively low, while RUNX3 expression was frequently down-regulated in both human HCC cell lines (91%) and tissues (90%).

Alterations in some tumor suppressor genes are due to LOH in HCC [17]. Similar to other tumor suppressor genes, some of the alterations in RUNX3 are due to the LOH of chromosome 1p36, where RUNX3 is located. Perhaps another mechanism for RUNX3 down-regulation is hypermethylation of the RUNX3 promoter region [13-16]. In a previous report, 30-40% of HCCs showed LOH of the RUNX3 gene and 40-80% showed promoter hypermethylation [28]. In agreement with these reports, RUNX3 down-regulation was detected in ~90% of HCC tissue specimens.

Conclusions

RUNX3 expression elicits serum starvation-induced apoptosis in HCC cells via the Bim-caspase pathway. Because RUNX3 expression is generally suppressed in HCC cell lines and tissues, loss of RUNX3 expression leads to tumorigenesis by escaping apoptosis.

Acknowledgements

We thank Tatsuya Fujikawa and Naoki Ueda for their valuable suggestions, and Noriaki Tanaka for providing the HCC tissues.

Author details

[1]Department of Gastroenterology and Hepatology, Okayama University Graduate School of Medicine and Dentistry, 2-5-1 Shikata-cho, Okayama 700-8558, Japan. [2]Department of Molecular Hepatology, Okayama University Graduate School of Medicine and Dentistry, 2-5-1 Shikata-cho, Okayama 700-8558, Japan. [3]Department of Gastroenterological Surgery, Transplant, and Surgical Oncology, Okayama University Graduate School of Medicine and Dentistry, 2-5-1 Shikata-cho, Okayama 700-8558, Japan.

Authors' contributions

HS conceived the design and drafted the manuscript. YN performed experiments. NT, ST, SN, MU, MM, MI and AT helped performing experiments for YN. SN, YK, KN, KK, HH, JT, HO and TY contributed for the collection of HCC tissues. YN performed immunohistochemical study. KY provides financial supports and participates in the discussion of the results. All authors read and approved the final manusctipt.

Competing interests

The authors declare that they have no competing interests.

Received: 10 August 2010 Accepted: 4 January 2011
Published: 4 January 2011

References

1. El-Serag HB, Rudolph KL: **Hepatocellular carcinoma: epidemiology and molecular carcinogenesis.** *Gastroenterology* 2007, **132(7)**:2557-2576.
2. Garcia M, Jernal A, Ward EM, M CM, Hao Y, Siegel RI, Thun MJ: **Global Cancer Facts & Figures 2007.** Society AC. Atlanta, GA; 2007.
3. Parkin DM, Bray F, Ferlay J, Pisani P: **Estimating the world cancer burden: Globocan 2000.** *Int J Cancer* 2001, **94(2)**:153-156.
4. El-Serag HB, Mason AC: **Rising incidence of hepatocellular carcinoma in the United States.** *N Engl J Med* 1999, **340(10)**:745-750.
5. Kremer-Tal S, Reeves HL, Narla G, Thung SN, Schwartz M, Difeo A, Katz A, Bruix J, Bioulac-Sage P, Martignetti JA, *et al*: **Frequent inactivation of the tumor suppressor Kruppel-like factor 6 (KLF6) in hepatocellular carcinoma.** *Hepatology* 2004, **40(5)**:1047-1052.
6. Kaposi-Novak P, Lee JS, Gomez-Quiroz L, Coulouarn C, Factor VM, Thorgeirsson SS: **Met-regulated expression signature defines a subset of human hepatocellular carcinomas with poor prognosis and aggressive phenotype.** *The Journal of clinical investigation* 2006, **116(6)**:1582-1595.
7. Shachaf CM, Kopelman AM, Arvanitis C, Karlsson A, Beer S, Mandl S, Bachmann MH, Borowsky AD, Ruebner B, Cardiff RD, *et al*: **MYC inactivation uncovers pluripotent differentiation and tumour dormancy in hepatocellular cancer.** *Nature* 2004, **431(7012)**:1112-1117.
8. Sicklick JK, Li YX, Melhem A, Schmelzer E, Zdanowicz M, Huang J, Caballero M, Fair JH, Ludlow JW, McClelland RE, *et al*: **Hedgehog signaling maintains resident hepatic progenitors throughout life.** *American journal of physiology* 2006, **290(5)**:G859-870.
9. Azechi H, Nishida N, Fukuda Y, Nishimura T, Minata M, Katsuma H, Kuno M, Ito T, Komeda T, Kita R, *et al*: **Disruption of the p16/cyclin D1/retinoblastoma protein pathway in the majority of human hepatocellular carcinomas.** *Oncology* 2001, **60(4)**:346-354.
10. Hu TH, Huang CC, Lin PR, Chang HW, Ger LP, Lin YW, Changchien CS, Lee CM, Tai MH: **Expression and prognostic role of tumor suppressor gene PTEN/MMAC1/TEP1 in hepatocellular carcinoma.** *Cancer* 2003, **97(8)**:1929-1940.
11. Tannapfel A, Busse C, Weinans L, Benicke M, Katalinic A, Geissler F, Hauss J, Wittekind C: **INK4a-ARF alterations and p53 mutations in hepatocellular carcinomas.** *Oncogene* 2001, **20(48)**:7104-7109.
12. Yamada T, De Souza AT, Finkelstein S, Jirtle RL: **Loss of the gene encoding mannose 6-phosphate/insulin-like growth factor II receptor is an early event in liver carcinogenesis.** *Proc Natl Acad Sci USA* 1997, **94(19)**:10351-10355.
13. Fujimoto Y, Hampton LL, Wirth PJ, Wang NJ, Xie JP, Thorgeirsson SS: **Alterations of tumor suppressor genes and allelic losses in human hepatocellular carcinomas in China.** *Cancer Res* 1994, **54(1)**:281-285.
14. Kawai H, Suda T, Aoyagi Y, Isokawa O, Mita Y, Waguri N, Kuroiwa T, Igarashi M, Tsukada K, Mori S, *et al*: **Quantitative evaluation of genomic instability as a possible predictor for development of hepatocellular carcinoma: comparison of loss of heterozygosity and replication error.** *Hepatology* 2000, **31(6)**:1246-1250.
15. Nishida N, Nagasaka T, Nishimura T, Ikai I, Boland CR, Goel A: **Aberrant methylation of multiple tumor suppressor genes in aging liver, chronic hepatitis, and hepatocellular carcinoma.** *Hepatology* 2008, **47(3)**:908-918.
16. Yang B, Guo M, Herman JG, Clark DP: **Aberrant promoter methylation profiles of tumor suppressor genes in hepatocellular carcinoma.** *Am J Pathol* 2003, **163(3)**:1101-1107.
17. Buendia MA: **Genetics of hepatocellular carcinoma.** *Semin Cancer Biol* 2000, **10(3)**:185-200.
18. Ito K, Liu Q, Salto-Tellez M, Yano T, Tada K, Ida H, Huang C, Shah N, Inoue M, Rajnakova A, *et al*: **RUNX3, a novel tumor suppressor, is frequently inactivated in gastric cancer by protein mislocalization.** *Cancer Res* 2005, **65(17)**:7743-7750.
19. Ito Y, Miyazono K: **RUNX transcription factors as key targets of TGF-beta superfamily signaling.** *Curr Opin Genet Dev* 2003, **13(1)**:43-47.
20. Hanai J, Chen LF, Kanno T, Ohtani-Fujita N, Kim WY, Guo WH, Imamura T, Ishidou Y, Fukuchi M, Shi MJ, *et al*: **Interaction and functional cooperation of PEBP2/CBF with Smads. Synergistic induction of the immunoglobulin germline Calpha promoter.** *J Biol Chem* 1999, **274(44)**:31577-31582.
21. Li QL, Ito K, Sakakura C, Fukamachi H, Inoue K, Chi XZ, Lee KY, Nomura S, Lee CW, Han SB, *et al*: **Causal relationship between the loss of RUNX3 expression and gastric cancer.** *Cell* 2002, **109(1)**:113-124.
22. Yamamura Y, Lee WL, Inoue K, Ida H, Ito Y: **RUNX3 cooperates with FoxO3a to induce apoptosis in gastric cancer cells.** *J Biol Chem* 2006, **281(8)**:5267-5276.
23. Araki K, Osaki M, Nagahama Y, Hiramatsu T, Nakamura H, Ohgi S, Ito H: **Expression of RUNX3 protein in human lung adenocarcinoma: Implications for tumor progression and prognosis.** *Cancer Sci* 2005, **96(4)**:227-231.
24. Ku JL, Kang SB, Shin YK, Kang HC, Hong SH, Kim IJ, Shin JH, Han IO, Park JG: **Promoter hypermethylation downregulates RUNX3 gene expression in colorectal cancer cell lines.** *Oncogene* 2004, **23(40)**:6736-6742.
25. Li J, Kleeff J, Guweidhi A, Esposito I, Berberat PO, Giese T, Buchler MW, Friess H: **RUNX3 expression in primary and metastatic pancreatic cancer.** *J Clin Pathol* 2004, **57(3)**:294-299.
26. Wada M, Yazumi S, Takaishi S, Hasegawa K, Sawada M, Tanaka H, Ida H, Sakakura C, Ito K, Ito Y, *et al*: **Frequent loss of RUNX3 gene expression in human bile duct and pancreatic cancer cell lines.** *Oncogene* 2004, **23(13)**:2401-2407.
27. Mori T, Nomoto S, Koshikawa K, Fujii T, Sakai M, Nishikawa Y, Inoue S, Takeda S, Kaneko T, Nakao A: **Decreased expression and frequent allelic inactivation of the RUNX3 gene at 1p36 in human hepatocellular carcinoma.** *Liver Int* 2005, **25(2)**:380-388.
28. Xiao WH, Liu WW: **Hemizygous deletion and hypermethylation of RUNX3 gene in hepatocellular carcinoma.** *World J Gastroenterol* 2004, **10(3)**:376-380.
29. Li X, Zhang Y, Qiao T, Wu K, Ding J, Liu J, Fan D: **RUNX3 Inhibits Growth of HCC Cells and HCC Xenografts in Mice in Combination With Adriamycin.** *Cancer Biol Ther* 2008, **7(5)**.
30. Ng IO, Chung LP, Tsang SW, Lam CL, Lai EC, Fan ST, Ng M: **p53 gene mutation spectrum in hepatocellular carcinomas in Hong Kong Chinese.** *Oncogene* 1994, **9(3)**:985-990.
31. Yano T, Ito K, Fukamachi H, Chi XZ, Wee HJ, Inoue K, Ida H, Bouillet P, Strasser A, Bae SC, *et al*: **The RUNX3 tumor suppressor upregulates Bim in gastric epithelial cells undergoing transforming growth factor beta-induced apoptosis.** *Mol Cell Biol* 2006, **26(12)**:4474-4488.
32. O'Connor L, Strasser A, O'Reilly LA, Hausmann G, Adams JM, Cory S, Huang DC: **Bim: a novel member of the Bcl-2 family that promotes apoptosis.** *Embo J* 1998, **17(2)**:384-395.
33. Puthalakath H, Huang DC, O'Reilly LA, King SM, Strasser A: **The proapoptotic activity of the Bcl-2 family member Bim is regulated by interaction with the dynein motor complex.** *Molecular cell* 1999, **3(3)**:287-296.
34. Brunet A, Bonni A, Zigmond MJ, Lin MZ, Juo P, Hu LS, Anderson MJ, Arden KC, Blenis J, Greenberg ME: **Akt promotes cell survival by phosphorylating and inhibiting a Forkhead transcription factor.** *Cell* 1999, **96(6)**:857-868.
35. Guo C, Ding J, Yao L, Sun L, Lin T, Song Y, Fan D: **Tumor suppressor gene Runx3 sensitizes gastric cancer cells to chemotherapeutic drugs by downregulating Bcl-2, MDR-1 and MRP-1.** *Int J Cancer* 2005.
36. Osaki M, Moriyama M, Adachi K, Nakada C, Takeda A, Inoue Y, Adachi H, Sato K, Oshimura M, Ito H: **Expression of RUNX3 protein in human gastric mucosa, intestinal metaplasia and carcinoma.** *Eur J Clin Invest* 2004, **34(9)**:605-612.
37. Torquati A, O'Rear L, Longobardi L, Spagnoli A, Richards WO, Daniel Beauchamp R: **RUNX3 inhibits cell proliferation and induces apoptosis by reinstating transforming growth factor beta responsiveness in esophageal adenocarcinoma cells.** *Surgery* 2004, **136(2)**:310-316.
38. Jin YH, Jeon EJ, Li QL, Lee YH, Choi JK, Kim WJ, Lee KY, Bae SC: **Transforming growth factor-beta stimulates p300-dependent RUNX3**